STATIC FRICTION MEASUREMENTS ON STEEL AGAINST UNCOATED AND COATED CAST IRON

P. Andersson[1], L. Kilpi[1], K. Holmberg[1], A. Vaajoki[1] and V. Oksanen[2]

[1] VTT Technical Research Centre of Finland, P.O.Box 1000, FI-02044 VTT (Espoo), Finland
[2] Tampere University of Technology, Department of Materials Science, P.O.Box 589, FI-33101 Tampere, Finland

ABSTRACT

Static friction is a phenomenon we may mainly consider as related to frictional joints within static mechanics. The step from static friction to tribological phenomena is, however, rather short, since at the onset of sliding in a mechanical contact, the static friction determines the initial resistance against motion. Static friction furthermore plays a role in contacts subjected to traction and fretting. Although being a phenomenon of short duration, the tribological phenomena during the transition from static friction to sliding friction may be of great importance for the operational life of the contact surfaces, particularly if the procedure is repeated for a sufficient number of times.

The present paper describes the principles of static friction measurements, details of the employed static friction tribometer and the results of measurements with unlubricated and lubricated sliding couples consisting of steel against uncoated and coated cast iron.

Keywords: Static friction, friction transitions, sliding friction, tribometer.

*Corresponding author: Peter Andersson (peter.andersson@vtt.fi)

INTRODUCTION

By definition, tribology is the science and technology of interacting surfaces in relative motion and of the practices related thereto [1]. Strictly taken, static friction as such is not covered by this definition, since traditionally static friction is included in the static mechanics, for example in the dimensioning of screw joints, shrink fits and pressure fits, in more developed machine components like clutches and parking brakes, and in belt drives, rope drives, wheels, shoes and other types of traction drive systems.

However, before even the slightest relative movement could commence in a mechanical contact intended for full or partial sliding motion, the tangential force acting in the contact has to pass the limiting friction force that forms the border between static and kinetic friction, and this again connects the static friction phenomenon to the field of tribology. A typical situation, in which the static friction precedes the onset of sliding in a contact, is when a shaft starts to rotate in a journal bearing.

Under static friction, the contact temperature equals the surrounding temperature, and hydrodynamic effects are absent. The difference between static and kinetic friction for a given sliding couple determines its tendency for stick-slip frictional behavior. Static friction is partly present in contacts subjected to fretting, furthermore in traction,

5

in which mechanical energy is transferred under partly static and partly kinetic (sliding) friction from a driving component to a driven component [2]. The dwelling time, i.e. the time elapse from the formation of a static contact until the onset of relative motion in the contact, can affect the magnitude of the coefficient of static friction, particularly under lubricated conditions.

When a static contact, loaded by a normal force Fn, evolves into a sliding contact, the limiting static friction force Fµ has been exceeded, and the coefficient of static friction (µs) can be established. The coefficient of static friction between a body and a plane can be experimentally determined, at certain accuracy, by tilting the plane to an angle α, at which the gravity starts to pull the body downwards along the inclined plane [2, 3]. The expression µ=tan α is valid for the limiting frictional conditions at which a body starts to slide along the plane. The above expression for the limiting friction has been developed into a model called the cone of friction. Load conditions, in which the ratio of the tangential and normal forces give angles smaller than α, are located within the cone of friction and are secured against sliding.

Another method for the experimental determination of the coefficient of static friction is to use a centrifugal force apparatus, in which the gravity causes the normal force and the centrifugal force the tangential force on the movable sample [4].

In the simplest measurements of the static friction force, a spring balance or an electronic force recording system is used for measuring the static friction force needed for the initial mobilization of a loaded test sample along a flat surface [2].

For a more precise determination of the coefficient of static friction, the static friction force is measured at increasing load until the

onset of relative motion between the contact surfaces, as recorded by force and displacement instrumentation. The normal force Fn should act directly on the static sample holder and sample, and if the static sample is above the movable sample, the normal force is preferably achieved by gravity and dead weights. The lower sample holder and sample must move along the plane that goes through the sliding contact, and for providing accurate measurements, the motion must take place without any friction. Bending moments of force on the movable sample are avoided by applying the tangential force at the plane that goes through the sliding contact, and by directing the static friction force through the center of gravity of the contact surface between the upper and lower sample. If the friction force is measured along a plane that lies above the contact surface, a momentum of force is formed from the forces and the distance between their action points, and part of the contact pressure due to the normal force is transferred from the trailing edge of the sample to the leading edge. Furthermore, the movement of the movable sample holder and sample must take place along the plane through the contact interface, in the direction of the tangential force, and it must be smooth and without external sliding friction.

The present work is an attempt to support the development of rope drives, by performing a set of measurements on the static friction between a steel wire slider and flat, smooth surfaces of eleven different materials.

MATERIALS AND METHODS

Equipment

The static friction measurements in the present work employed an in-house built device called the VTT Static Friction Tribometer, see Figure 1. The tribometer casing consisted of an upper deck with two

support columns bolted onto a heavy plate made from cast iron. The upper deck hosed the holder for the static sample, or the upper test sample, which was loaded by dead weights and able to move in the vertical direction. A horizontally movable frame beneath the upper deck hosed the lower or movable test sample. For measuring the static friction force, the movable frame was pulled horizontally by a pneumatic actuator equipped with a force transducer.
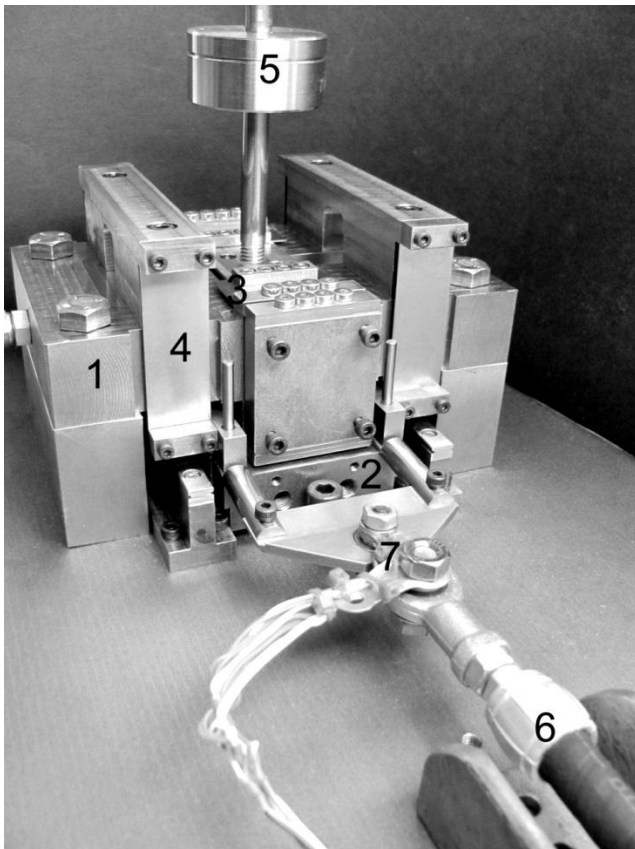
Fig. 1. The VTT Static Friction Tribometer. Upper deck (1), movable frame with the lower sample (2), suspension springs for the upper sample holder (3), suspension springs for the movable frame (4), weights on a loading rod (5), pneumatic actuator (6) and force transducer (7). The displacement transducer was located on the opposite side of the tribometer.

The upper test sample, which was a piece of steel wire that had been bent into U-shape, was mounted in a holder in a vertical channel through the upper deck. The holder was suspended and guided by a pair of horizontally orientated leaf spring blades in the direction of motion of the movable sample, see Figure 2. The leaf springs allowed the holder to move vertically for the short distance needed when applying a load in a test, however providing determined, horizontal positioning of the upper and lower ends of the upper sample holder. The blades had been laser-cut from a 0.5 mm thick sheet of spring steel. One of the blades had been rigidly attached by screw joints on the upper side of the upper deck and the upper sample holder, and the other blade on the lower side of the deck and holder. When loading the upper sample by the dead weights, the initial air gap between the upper and lower sample was closed and the entire set-up was subjected to minor compression, and due to this the spring blades were subjected to a weak deflection. A pre-stress in the length direction of the spring blades removed any slacken in the blades however still allowing the deflection of the blades.

The lower test sample, which was a disc, was mounted in a horizontally movable frame. The movable frame was suspended by four vertical leaf spring blades (Fig. 1). The suspension blades allowed the frame to move horizontally, and without internal friction, for the short distance needed for the friction force measurements, in the correct direction, and without frictional losses. The blades had been rigidly mounted by screw joints to the upper deck and to the movable frame, thus being subjected to deflection into a very weak S-shape when the frame was moved from its resting position.

7
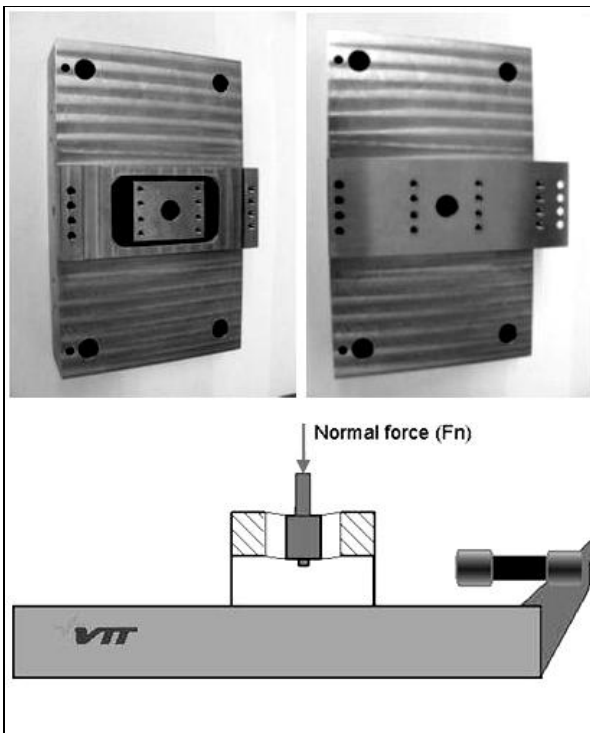
Fig. 2. Suspension leaf springs for the upper sample holder; the upper sample holder in the upper deck (upper left image), the spring blade placed above the upper sample holder (upper right image) and the principle for spring blade suspension during loading by the normal force (lower image).

In the friction force measurements, an increasing tangential force was applied on the movable frame until motion could be determined by displacement measurements. The tangential force was achieved by a pneumatic actuator without sliding friction. The function of this particular type of pneumatic actuator was to create a tensile force when pressurized by air. The tangential force was measured by strain gages on two thin steel sections mounted between two spherical joints, between the actuator and the movable frame. In order to allow measurements without interference by frictional torque effects, the tangential force from the actuator was designed to horizontally intersect the contact spot of the friction couple. The position of the movable

test disc frame in the direction of the motion was recorded by means of a non-contacting displacement transducer (NCDT) based on the eddy-current effect.

Test specimens and sample holders

The tests were performed with a bent, U-shaped steel wire against an uncoated or coated cast iron disc (Fig. 3).
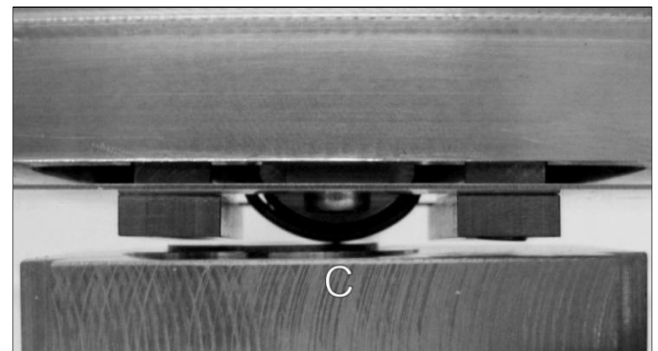
Fig. 3. Contact geometry of the test set-up consisting of a U-shaped steel wire and a cast iron disc. The contact between the steel wire slider and the disc sample is seen above the letter "C". In this image, the direction of motion of the disc sample in a test situation was to the right.

The steel wire samples were produced from $\varnothing$ 1.4 mm steel wire, which was pre-shaped on a mandrel for an outer radius of curvature of 11 mm, and mounted on a similarly curved support on a holder. According to the manufacturer, the steel wire had been drawn from non-alloyed steel with a pearlitic microstructure and had a tensile strength of 1700 N/mm2. The wire was uncoated and had a surface roughness of Ra=0.30 µm and Rsk=-1.0 when measured by VTT in the length direction of the wire, using a diamond stylus profilometer. The direction of the steel wire in the contact area coincided with the direction of the friction force and motion. A new steel wire was used for each test series.

Table 1 presents the sliding surface materials of the disc samples investigated, which represent 11 different types of uncoated and thermal spray coated cast iron. The surface roughness Ra and Rsk values of the sliding surfaces after flat grinding, lapping and polishing are included in the Table. The diameter of the uncoated discs was 24 mm and that of the coated ones 40 mm. In the test, the cast iron disc was radially attached to the sample holder. For each test series, the disc was re-positioned in order to introduce a new test spot.

The lubricant for the lubricated tests was an additive-free, paraffinic vaseline (petrolatum) with a melting point around 80 ℃.

Table 1. Sliding surface materials of the disc samples investigated.

Code	Designation	Tensile strength[1] [N/mm²]	Surface roughness[2]	
			Ra [µm]	Rsk [-]
Ferritic SG iron	Nodular cast iron - also known as spheroidal graphite cast iron (SG iron) or ductile cast iron - with a solution strengthened ferritic microstructure.	600	0.15	-1.1
Pearlitic SG iron	Nodular cast iron with a mainly pearlitic microstructure.	700	0.244	-2.1
Grey cast iron	Molybdenum-alloyed grey or lamellar cast iron.	330	0.36	-0.7
ADI	Austempered ductile cast iron (ADI).	1000	0.07	-2.0
P/F-CDI (pearlitic-ferritic chill-cast SG iron)	Chill-cast nodular cast iron with a pearlitic matrix with dendritic, lamellar cementite precipitations and bull's-eye ferrite.	N.A.	0.13	-1.1
P-CDI (pearlitic chill-cast SG iron)	Chill-cast nodular cast iron with a pearlitic matrix with dendritic, lamellar cementite precipititations and very low ferrite content.	N.A.	0.11	-1.4
CrC-TS1	Cast iron disc that had been thermal spray coated with a commercial, thermal spray, chromium carbide (CrC) cermet based coating.	N.A.	0.02	-1.5
WC-TS2	Cast iron disc that had been thermal spray coated with a commercial, thermal spray, tungsten carbide (WC) cermet based coating.	N.A.	0.02	-1.9
Mo-TS3	Cast iron disc that had been thermal spray coated with a commercial, thermal spray, molybdenum (Mo) based coating.	N.A.	0.18	-2.3
CrC-TS4	Cast iron disc that had been thermal spray coated with an experimental, thermal spray, chromium carbide (CrC) cermet based coating.	N.A.	0.01	-2.0
VC-TS5	Cast iron disc that had been thermal spray coated with an experimental, thermal spray, vanadium carbide (VC) cermet based coating.	N.A.	0.07	-1.8

[1] Tensile strength values obtained from the manufacturer.
[2] Surface roughness values as measured by VTT using a diamond stylus instrument.

Experimental procedure

The present experiments were carried out at a temperature of 22±1 °C, in room air of 50±5% relative humidity. At least two series of unlubricated tests and two series of lubricated tests with normal forces increasing from zero to 96 N and back were performed on each disc material, as shown in the test sequence of Fig. 4. Before testing, the samples were ultrasonically cleaned in petroleum ether. The thickness of the petrolatum layer applied on the disc was about 0.5 mm. The petrolatum layer was applied before the first friction force measurement on a specific contact spot, and it was not renewed during the test series that was performed on the same contact spot.

When a pair of samples had been installed in the tribometer, the clearance between the samples was adjusted to be about 1 µm in the vertical direction, i.e. until the gap between the upper and lower sample was almost closed after a set of dead weights had been applied on the upper sample holder. After this, the friction force measurements were performed at the chosen normal force, which was obtained by adding dead weights on the upper sample holder.

In each test cycle with a new steel wire against a new contact spot on the cast iron sample, the friction measurements were performed under loads increasing from zero to 96 N, decreasing back to zero and increasing to 96 N, for finally decreasing back to zero, all in steps of 9.6 N. Between each measurement, the load was removed and the lower sample was allowed to return to its resting position, see Fig. 4.

Within 20 seconds after the application of the chosen load, the air pressure to the tangential force actuator was slowly increased. When the limiting friction had been exceeded and the test disc frame begun to move, as

indicated by a change in the signal from the NCDT (Fig. 5), the air pressure was manually lowered to zero.
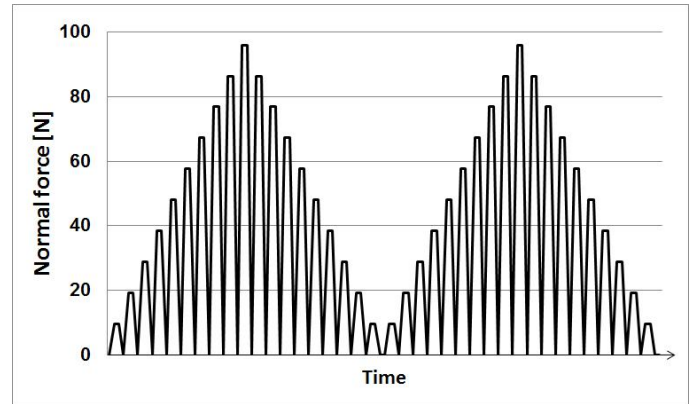
Fig. 4. Illustration of the loading sequence in the static friction measurements; the load levels were 9.6, 19.2, 28.8, 38.4, 48.0, 57.6, 67.2, 76.8, 86.4 and 96.0 N.
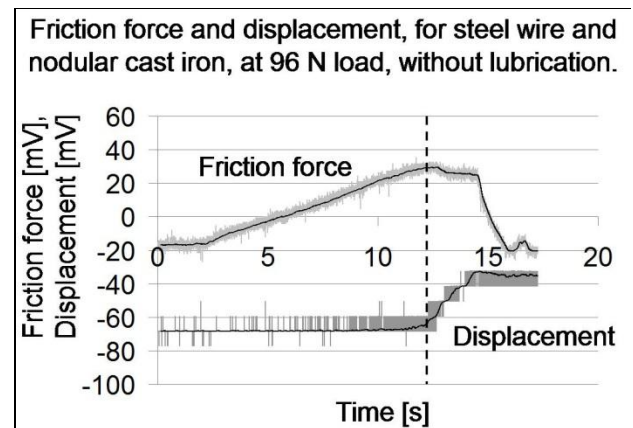
Fig. 5: Example of force and displacement readings in a static friction measurement. The dotted, vertical line indicates the limiting friction force, i.e. the value of relevance in the present study.

Calibrations

The spring constant for the leaf springs of the upper specimen holder was determined by loading the holder assembly, without a lower sample, by a set of dead weights and by measuring the corresponding vertical displacements by using a Heidenhain linear

variable displacement transducer (LVDT). The spring constant thus determined was 0.3 N/µm and practically uniform within the present deflection ranges.

In order to evaluate the deflection of the leaf springs of the upper specimen holder, the test set-up was loaded by a set of dead weights, and the corresponding vertical displacements were measured with the LVDT. At 100 N normal force, the leaf spring deflection due to elastic deformation of the samples and tribometer parts was 12 µm.

The reduction in normal force, by the deflection of the leaf springs of the upper specimen holder during the tests, was calculated from the vertical displacements and the spring constants; the normal force was 94…96% of the load on the samples, and this was considered in the friction coefficient calculations. Throughout the present work, only corrected normal forces are reported. Owing to the low magnitude of the vertical deflection in comparison with the free length of the spring steel suspension blades, vertical forces due to the cosine rule can be neglected.

The tangential force transducer was calibrated in its horizontal working position by loading it using a set of dead weights and a string via a pulley with a ball bearing. The measurements showed a linear signal response of 1 mV / 0.52 N for forces up to 30 N.

Using the actuator, the non-contacting displacement transducer, by which the horizontal displacement of the movable frame was measured during the tests, was cross-calibrated against the pre-calibrated LVDT. The comparison showed that the NCDT gave its nominal signal response, or 1 mV/µm.

In order to evaluate the influence of the deflection of the four leaf springs carrying the movable frame during the tests, on the friction force reading, the spring constant for the leaf springs was determined by loading the spring-and-frame assembly by a range of tangential forces from the pneumatic actuator, and by measuring the corresponding horizontal displacements by using the LVDT. The spring constant of the set of blades was 0.015 N/µm horizontal movement and practically uniform within the present deflection range.

The reduction in the friction force readings, by the deflection of the leaf springs of the movable lower specimen frame, was calculated from the horizontal displacements and the spring constant; the recorded friction force reading was more than 99% of the actual friction force on the samples. Owing to the low magnitude of horizontal deflection in comparison with the free length of the suspension blades, any horizontal reaction forces due to the cosine rule, from the normal force on the test specimens, can be neglected.

RESULTS

Steel against ferritic SG iron

Graphs showing the coefficients of static friction for steel wire against the ferritic SG iron under unlubricated and petrolatum-lubricated conditions, respectively, are presented in the Figs. 6 and 7. In these and the subsequent friction graph images, "First up" refers to the first load increase from 0 N to 96 N, "First down" refers to the first load decrease from 96 N to 0 N, "Second up" refers to the second load increase from 0 N to 96 N, and "Second down" refers to the second load decrease from 96 N to 0 N. Micrographs showing wear scars on the samples after the test cycles with steel against ferritic SG iron are presented in the Figs. 8 and 9.
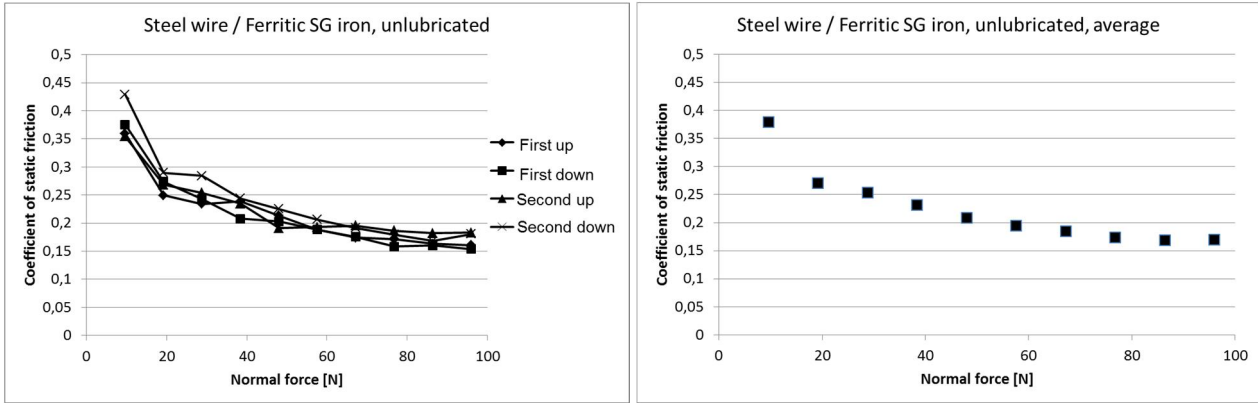
Fig. 6. Coefficients of static friction for an unlubricated contact with steel wire against ferritic SG iron. The average value at 38.4...96 N load (26 measurement points) was µs=0.190±0.025.
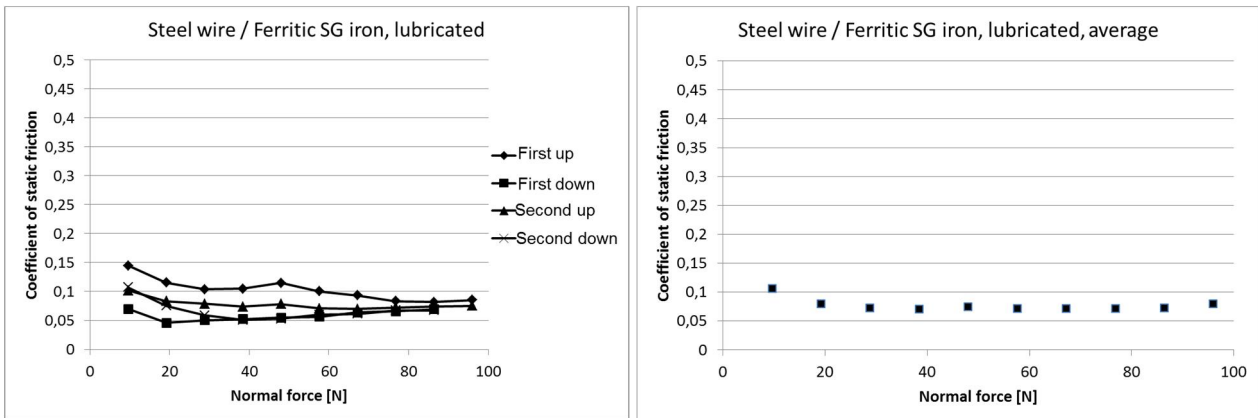
Fig. 7. Coefficients of static friction for a lubricated contact with steel wire against ferritic SG iron. The average value at 38.4...96 N load (26 measurement points) was µs=0.073±0.016.
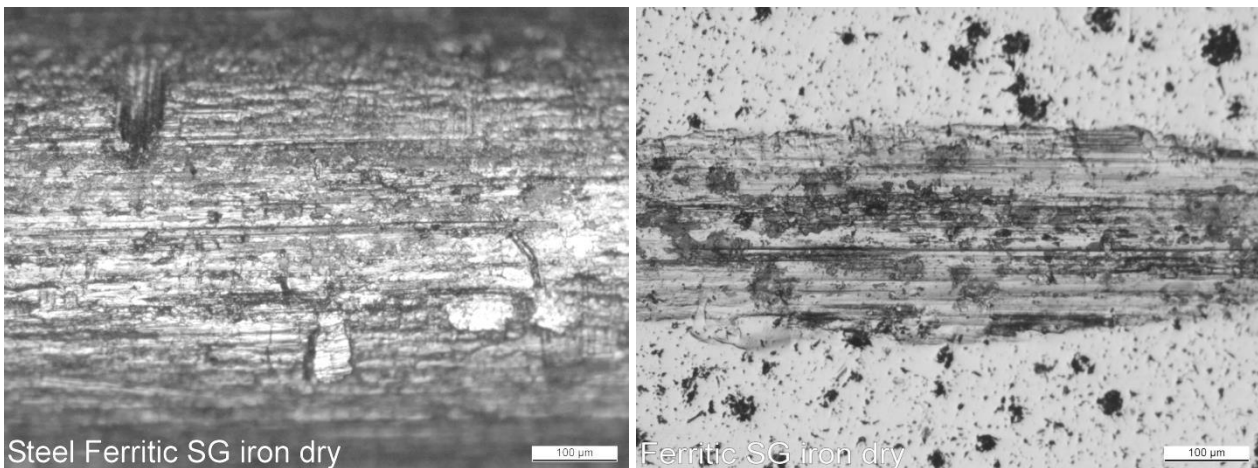
Fig. 8. Wear scar on a (left image) steel wire and the (right image) corresponding ferritic SG iron disc sample after the test cycle without lubrication. The direction of motion of the steel wire sample was horizontal in the images.
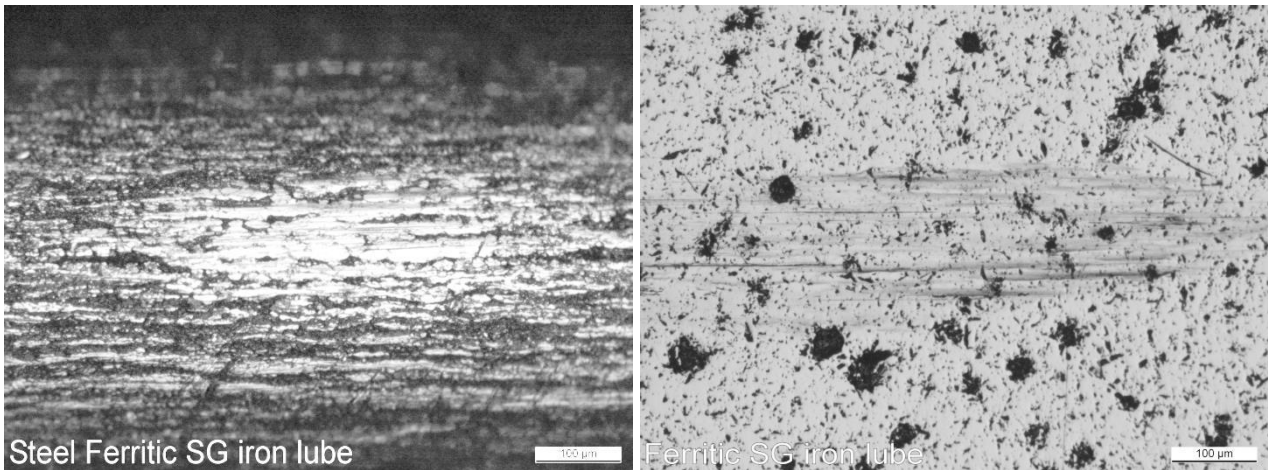
Fig. 9. Wear scar on a (left image) steel wire and the (right image) corresponding ferritic SG iron disc sample after the test cycle with lubrication by petrolatum. The direction of motion of the steel wire sample was horizontal in the images.

Unlubricated contact of steel against ferritic nodular cast iron

With steel wire against ferritic nodular cast iron of Rm=600 N/mm2 tensile strength, the coefficient of static friction under unlubricated conditions was significantly higher at low loads than at higher loads. The coefficient of static friction decreased until the normal force increased to approximately 70 N, above which the coefficient of static friction remained almost constant. Within the normal force range 38.4...96 N, the average value for the coefficient of static friction under unlubricated conditions was µs=0.18. With a disc made from the ferritic nodular cast iron, the difference between the frictional values in the two load increasing cycles in comparison with those of the two load decreasing cycles was very small.

During the 38 dry measurements under normal forces of 10…100 N, a sliding surface had been formed on the steel wire. The sliding surface on the steel wire sample had become slightly smoothened and shining. The corresponding sliding surface on the ferritic cast iron disc was covered by tiny scratches in the direction of motion of the steel wire, which means that during the unlubricated measurements, neither of the two counter surfaces had suffered from extensive alterations on their sliding surfaces.

Lubricated contact of steel against ferritic nodular cast iron

When the steel wire and ferritic nodular cast iron couple had been lubricated with petrolatum, the average value for the coefficient of static friction decreased to µs=0.07. Within the entire normal force range, the average values corresponding to the ten load levels were significantly lower in the lubricated tests. With lubrication by petrolatum, the difference between the frictional values in the two load increasing cycles (µs=0.090 on an average) and the two load decreasing cycles (µs=0.063 on an average) was significant, probably due to more beneficial boundary lubrication when the load was reduced.

The sliding surface formed on the steel wire sample during the lubricated measurements was more intensively polished, however on a smaller area, than in the dry tests with the same material combination. The wear mark on the ferritic cast iron disc only revealed tiny scratches or shallow grooves.

Steel against pearlitic nodular cast iron

Graphs showing the coefficients of static friction for steel wire against the pearlitic nodular cast iron at 9.6…96 N normal force, under unlubricated and petrolatum-lubricated conditions, respectively, are presented in the Figs. 10 and 11. Photomicrographs showing wear scars on the samples after the test cycles are presented in the Figs. 12 and 13. Two cross-sections across the sliding track of one of the tested pearlitic SG iron disc samples after a test cycle without lubrication are presented in Figure 14.
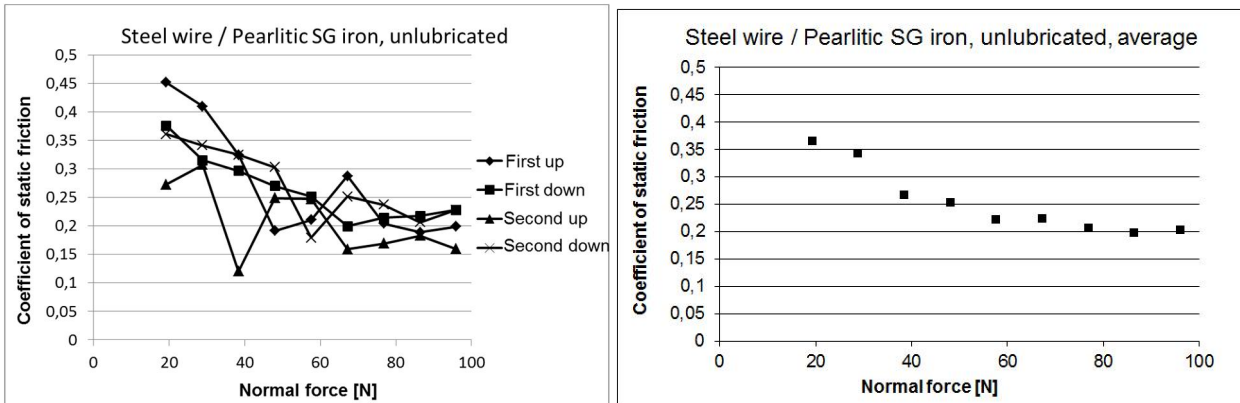
Fig. 10. Coefficients of static friction for an unlubricated contact with steel wire against pearlitic SG iron at 10...100 N load. The average value at 38.4...96 N load (26 measurement points) was $\mu s=0.225\pm0.051$.
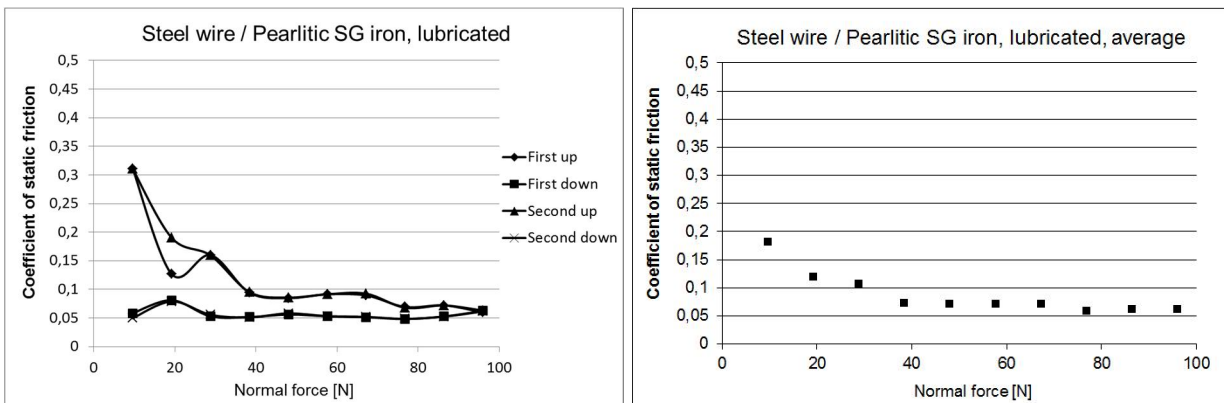
Fig. 11. Coefficients of static friction for a lubricated contact with steel wire against pearlitic SG iron. The average value at 38.4...96 N load (26 measurement points) was $\mu s=0.067\pm0.024$.
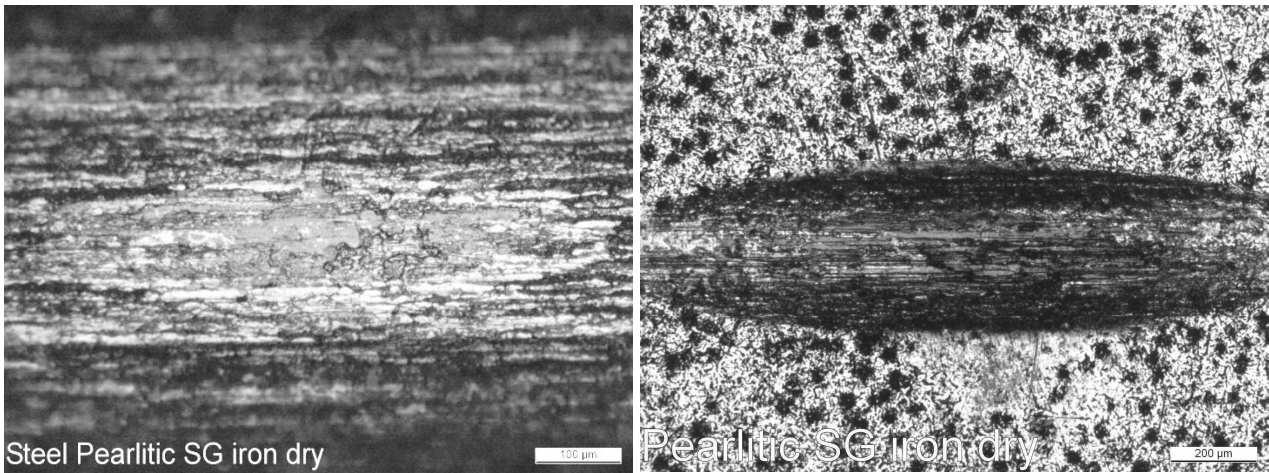
Fig. 12. Wear scar on a (left image) steel wire and the (right image) corresponding pearlitic nodular cast iron disc sample after the test cycle without lubrication. The direction of motion of the steel wire sample was horizontal in the images.
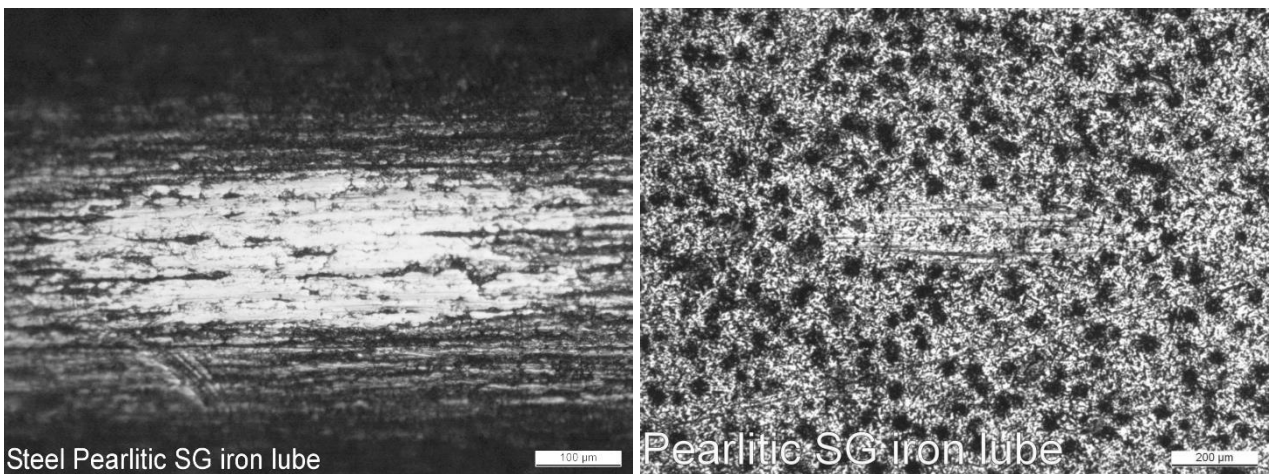
Fig. 13. Wear scar on a (left image) steel wire and the (right image) corresponding pearlitic SG iron disc sample after the test cycle with lubrication. The direction of motion of the steel wire sample was horizontal in the images.
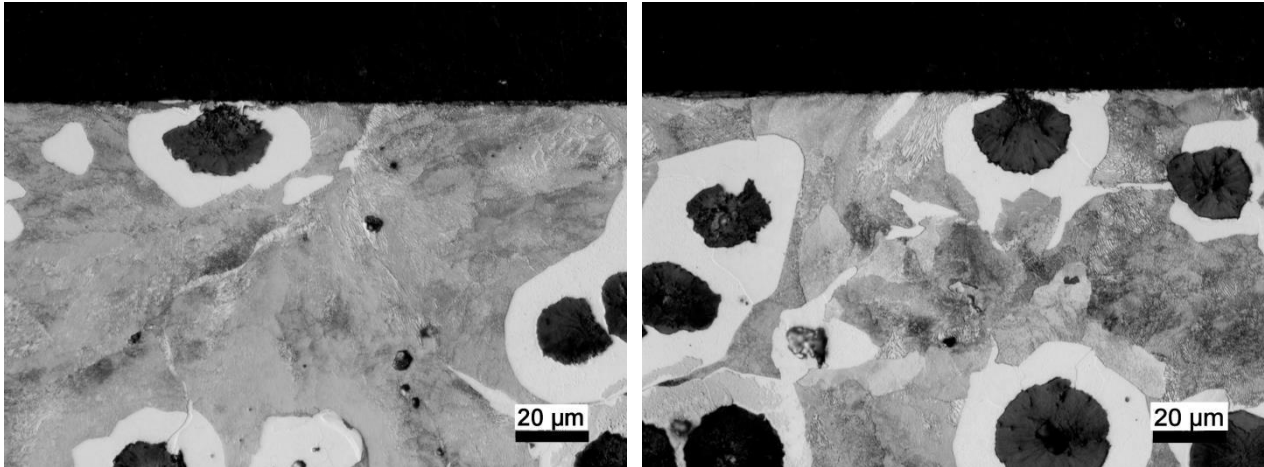
Fig. 14. Cross-section views of the sliding track of a pearlitic SG iron disc sample after a test cycle without lubrication. The direction of motion of the steel wire sample was horizontal in the image. The left image shows a deformed graphite sphere from which no graphite seems to have been extruded. The right image shows a deformed graphite sphere from which part of the graphite apparently has been extruded and has formed a solid lubricant film on the sliding surface.

Unlubricated contact of steel against pearlitic nodular cast iron

The unlubricated measurements with steel wire and a disc made from the pearlitic nodular cast iron with a tensile strength of Rm=700 N/mm2 showed that the average value for the coefficient of static friction was µs=0.22 at the normal force range 38.4...96 N. At lower loads, the coefficient of static friction decreased with an increase in the load, from µs=0.36 at about 20 N load, to µst=0.22 at about 60 N load. The frictional values at the two load increasing cycles and the two load decreasing cycles contain some scatter in the results rather than systematic differences between the friction force during load increase and decrease.

The sliding surfaces, which had been formed on the steel wire and the pearlitic nodular cast iron samples during the unlubricated measurements, were rather rough. The contact surface on the steel wire sample was shining however with scratches in the sliding direction. The cast iron contact surface was dark and probably covered by a mixture of graphite and oxidized ferrous transfer layer fragments with scratches in the direction of sliding. The extrusion of graphite from the graphite spheres of the cast material is obvious from Fig. 14. With respect to the sliding distance elapsed, the surface alterations were rather strong, which is in agreement with the high coefficient of friction recorded in the unlubricated conditions and the relatively high initial surface roughness of the cast iron disc.

Lubricated contact of steel against pearlitic nodular cast iron

In the lubricated measurements with steel wire and the pearlitic nodular cast iron, the average value for the coefficient of static friction was µs=0.07 at the normal force range 38.4...96 N. The difference between frictional values during the two load increasing cycles and the two load decreasing cycles was significant, with a particularly low and stable level for the coefficient of static friction when going from higher normal forces towards lower ones; During the two cycles of increasing normal force, the average value for

the coefficient of static friction was µs=0.12 for the entire normal force range, i.e. 9.6…96 N. The corresponding value during the two cycles of decreasing normal force was µs=0.06, which indicates beneficial boundary lubrication of the tribocouple during the unloading cycle.

Steel against grey cast iron

Graphs showing the coefficients of static friction for steel wire against grey cast iron at 9.6…96 N load, under unlubricated and petrolatum-lubricated conditions, respectively, are presented in the Figs. 15 and 16, and photomicrographs showing wear scars on the samples after the test cycles are presented in the Figs. 17 and 18.
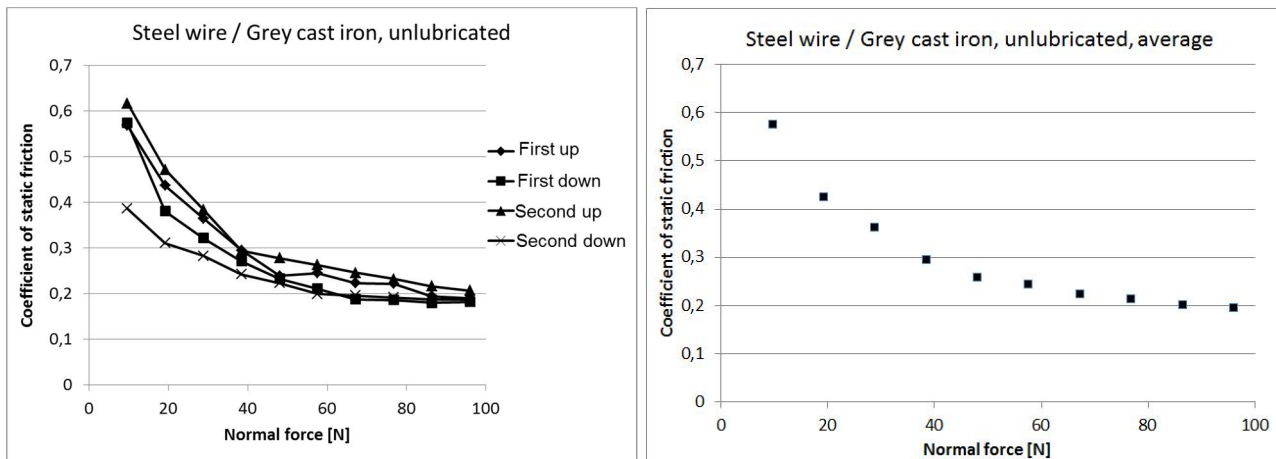
Fig. 15. Coefficients of static friction for unlubricated contact with steel wire against grey cast iron. The average value at 38.4...96 N load (26 measurement points) was µs=0.233±0.038.
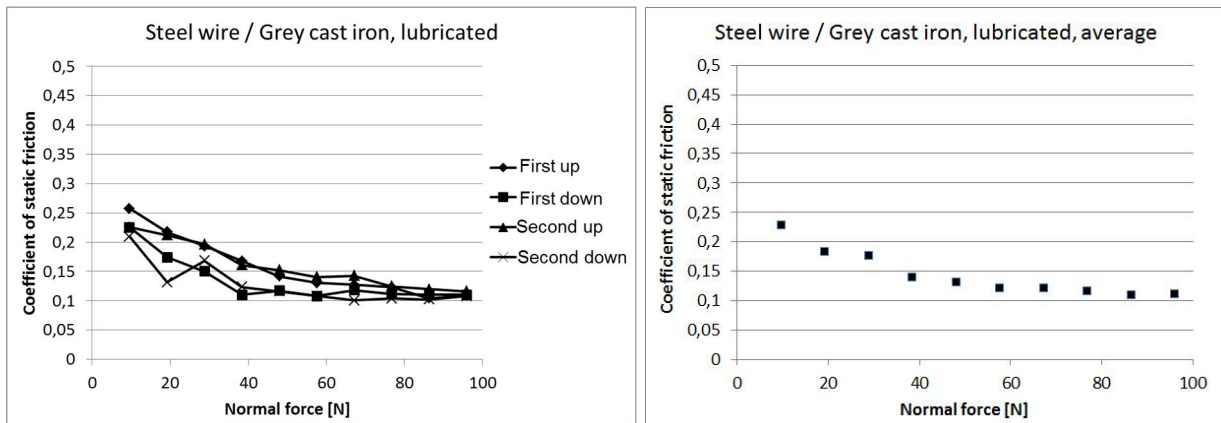
Fig. 16. Coefficients of static friction for a lubricated contact with steel wire against grey cast iron. The average value at 38.4...96 N load (26 measurement points) was µs=0.122±0.018.
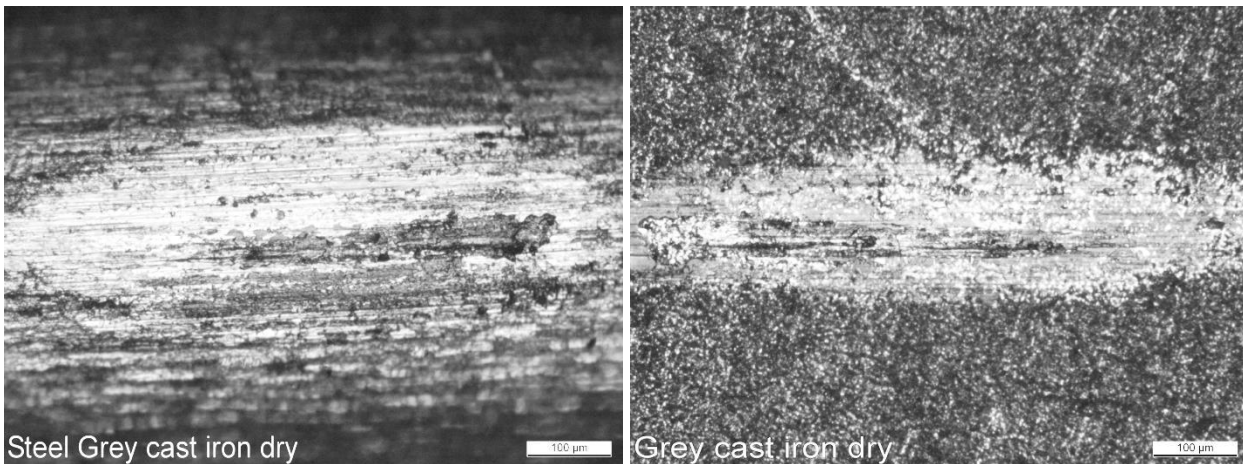
Fig. 17. Wear scar on a (left image) steel wire and the (right image) corresponding grey cast iron disc sample after the test cycle without lubrication. The direction of motion of the steel wire sample was horizontal in the images.
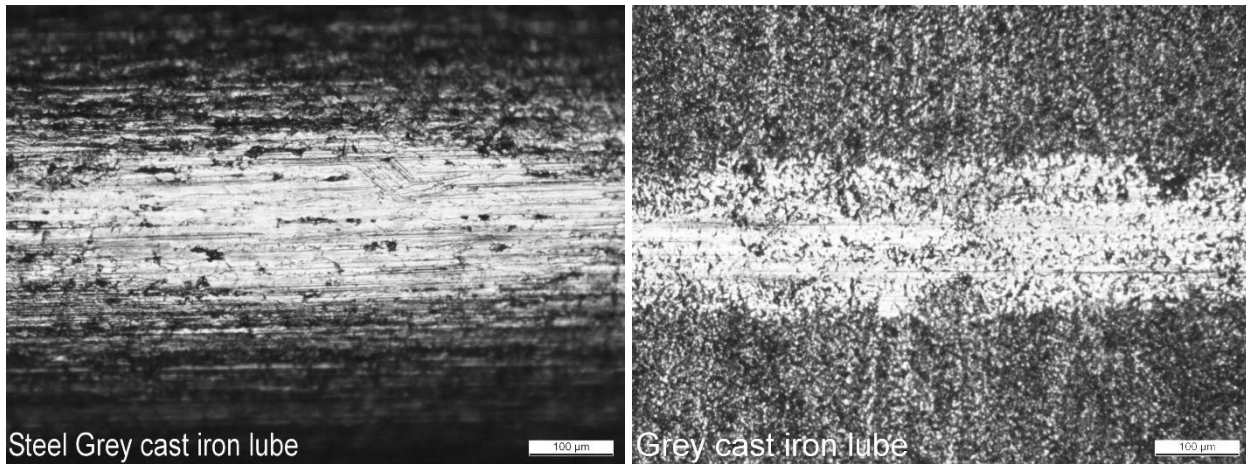
Fig. 18. Wear scar on a (left image) steel wire and the (right image) corresponding grey cast iron disc sample after the test cycle with lubrication by petrolatum. The direction of motion of the steel wire sample was horizontal in the images.

Unlubricated contact of steel against Mo-alloyed grey cast iron

In the dry tests, the level of the coefficient of static friction for steel and grey cast iron was close to that in the tests with the nodular cast irons. The decrease in the coefficient of friction with load was strong for normal forces up to 70 N, after which a stable level occurred. At the normal force range 38.4...96 N, the average value for the coefficient of static friction was $\mu_s=0.23$, which is on the same level as for the pearlitic nodular cast iron and slightly higher than for the ferritic nodular cast iron. The relatively high arithmetic average surface roughness of Ra=0.36 µm of the cast iron disc, may be partly responsible for the high coefficients of static friction during the unlubricated measurements. The influence of the load-increasing-and-decreasing cycles, i.e. the preceding loads, on the coefficient of static friction at the respective load levels was small during the unlubricated measurements.

18

The wear scars formed on the steel wire and cast iron disc in the unlubricated tests revealed irregular patches of transfer layers and a high density of tiny scratches in the direction of the measurements.

Lubricated contact of steel against Mo-alloyed grey cast iron

Lubrication by paraffinic petrolatum had a clear effect on the coefficient of static friction for steel against lamellar cast iron, which was only µs=0.12 as an average value in the normal force range 38.4...96 N. The coefficient of static friction showed a decrease with increasing normal force up to 50 N. Certain degree of scatter in the coefficient of static friction was recorded at

the different load levels, and this probably indicates more or less beneficial boundary lubrication conditions, due to variations in the preceding sliding events, and contact condition changes arising thereof.

Steel against ADI

Graphs showing the coefficients of static friction for steel wire against the ADI at 9.6…96 N load, under unlubricated and petrolatum-lubricated conditions, respectively, are presented in the Figs. 19 and 20, and photomicrographs showing wear scars on the samples after the test cycles are presented in the Figs. 21 and 22.
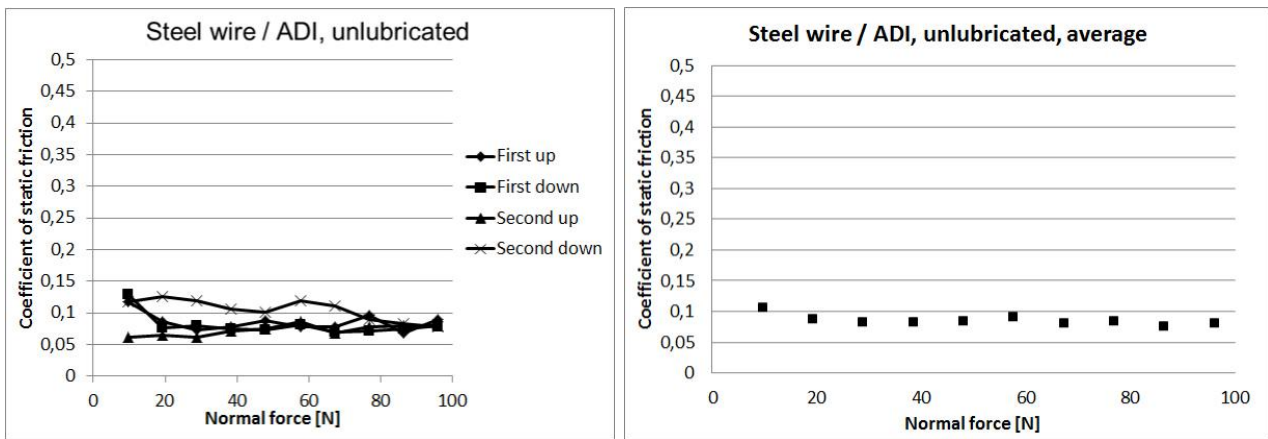
Fig. 19. Coefficients of static friction for unlubricated contact with steel wire against ADI. The average value at 38.4...96 N load (26 measurement points) was µs=0.083±0.013.
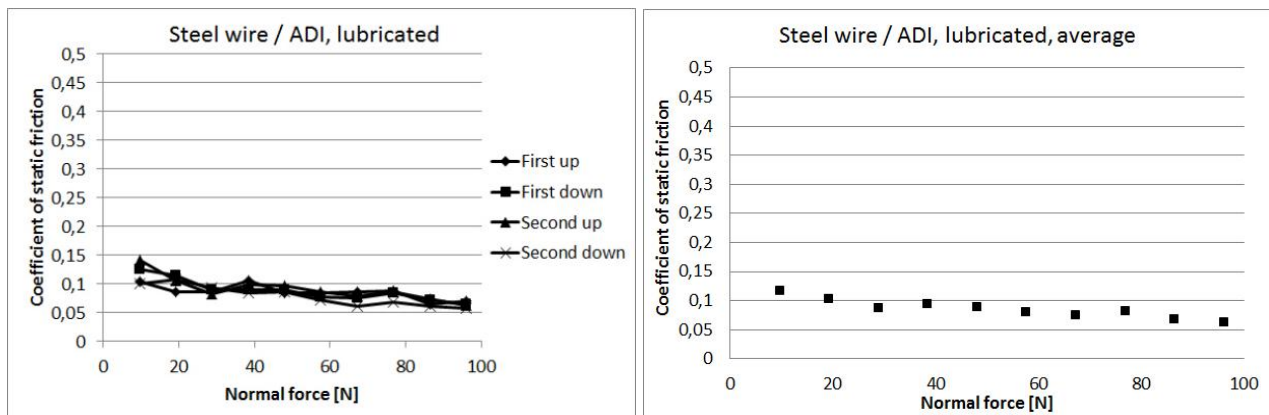
Fig. 20. Coefficients of static friction for a lubricated contact with steel wire against ADI. The average value at 38.4...96 N load (26 measurement points) was µs=0.079±0.012.
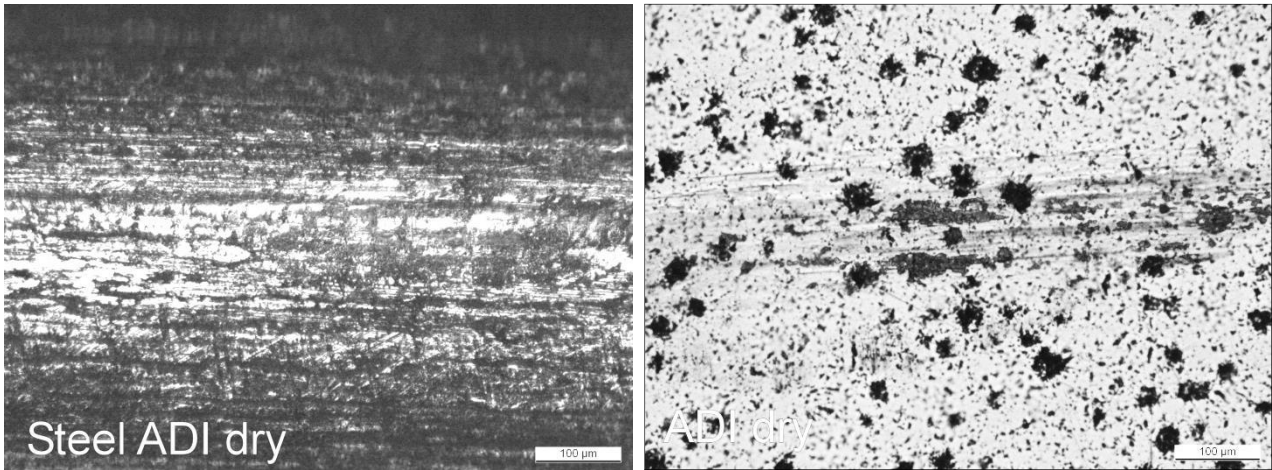
Fig. 21. Wear scar on the (left image) steel wire and the (right image) corresponding ADI disc sample after the test cycle without lubrication. The direction of motion of the steel wire sample was horizontal in the images.
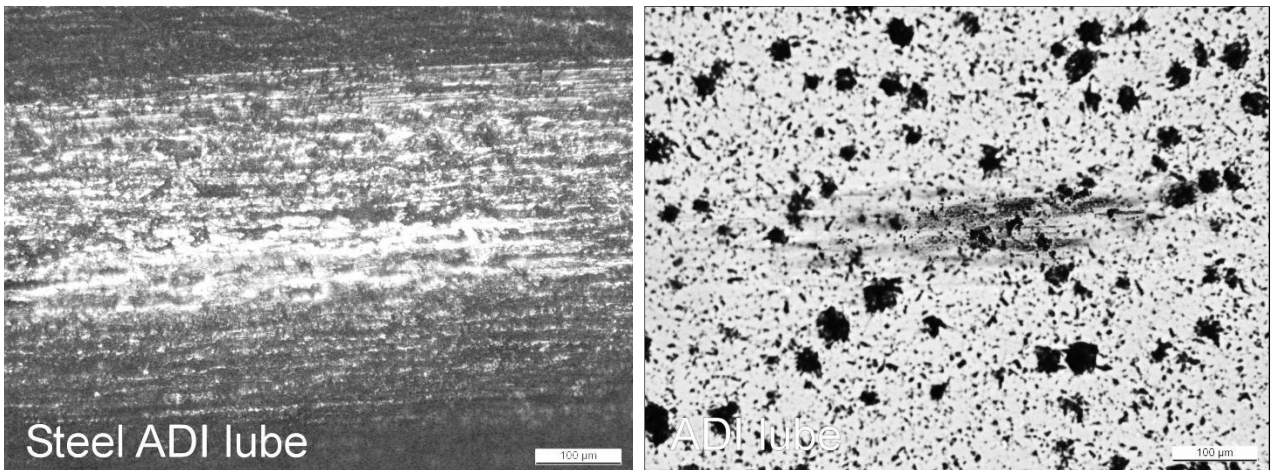
Fig. 22. Wear scar on the (left image) steel wire and the (right image) corresponding ADI disc sample after the test cycle with lubrication. The direction of motion of the steel wire sample was horizontal in the images.

Unlubricated contact of steel against austempered ductile cast iron

Under unlubricated conditions, the coefficient of static friction for steel against ADI was among the lowest within the present study, or µ=0.083, and quite stable over the load levels and number of contacting events. The low coefficient of friction is in good agreement with the low degree of surface alterations on the steel wire and ADI surfaces, indicating very low degrees of plastic deformation and

adhesive wear. The low degree of plastic deformation of the contact surfaces reflects the fairly high hardness of the two materials, while the low degree of adhesive wear reflects a solid-lubricating effect of the graphite spheres in spite of the hard metallic matrix.

Lubricated contact of steel against austempered ductile cast iron

With lubrication, the coefficient of static friction (µ=0.079) was slightly reduced and

the wear or deformation of the steel and ADI surfaces was reduced. Also in this case, the coefficient of friction showed a fairly good stability over the number of contact events, although a small decrease could be noticed with higher loads. In terms of the coefficient of static friction, the steel-against-ADI combination can be regarded as rather insensitive to the lubricating conditions within the range studied.

Steel against P/F-CDI

Graphs showing the coefficients of static friction for steel wire against the pearlitic-ferritic chill-cast SG iron at 9.6…96 N load, under unlubricated and petrolatum-lubricated conditions, respectively, are presented in the Figs. 23 and 24, and micrographs showing wear scars on the samples after the test cycles are presented in the Figs. 25 and 26.
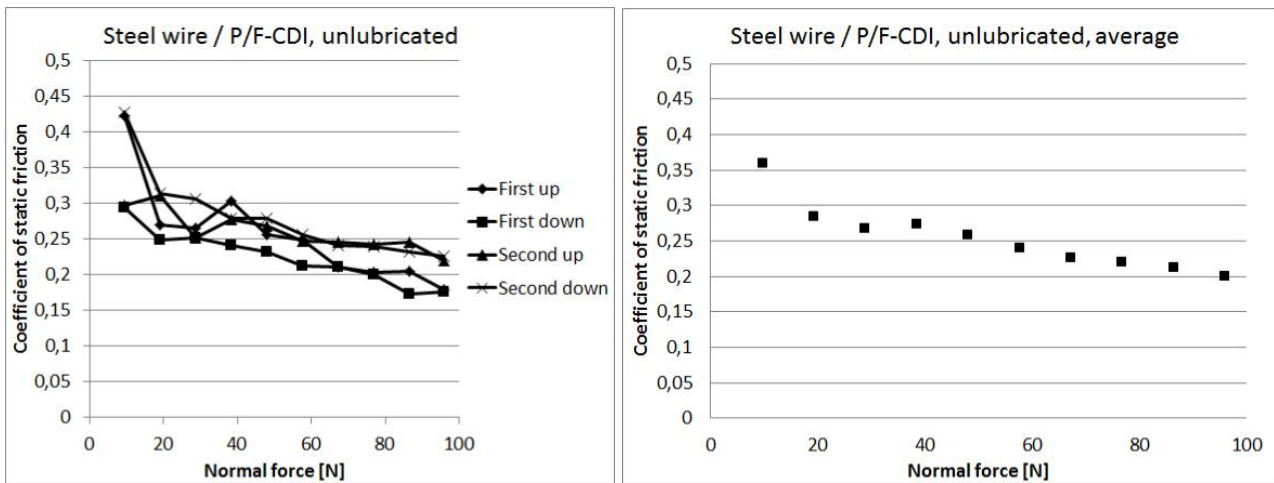
Fig. 23. Coefficients of static friction for unlubricated contact with steel wire against pearlitic-ferritic chill-cast SG iron. The average value at 38.4...96 N load (26 measurement points) was $\mu s = 0.234 \pm 0.032$.
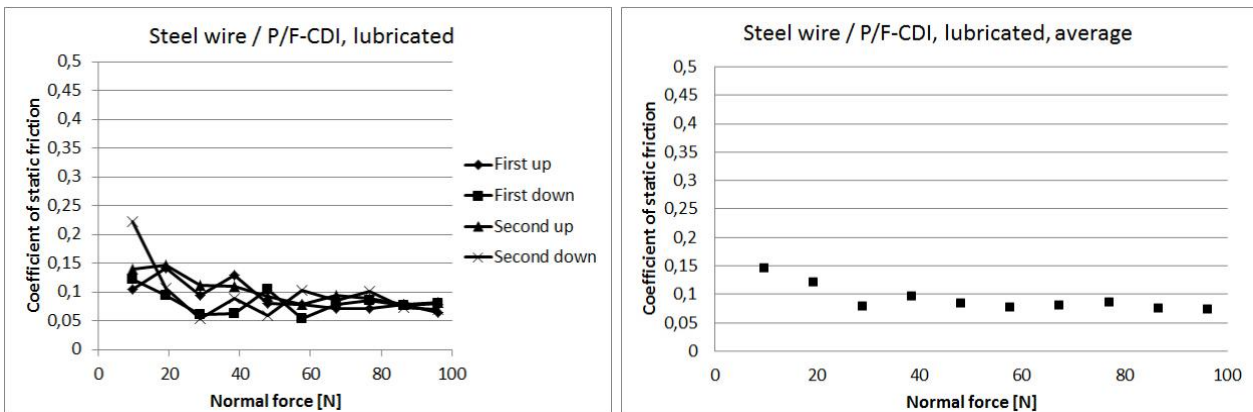
Fig. 24. Coefficients of static friction for a lubricated contact with steel wire against pearlitic-ferritic chill-cast SG iron. The average value at 38.4...96 N load (26 measurement points) was $\mu s = 0.083 \pm 0.016$.
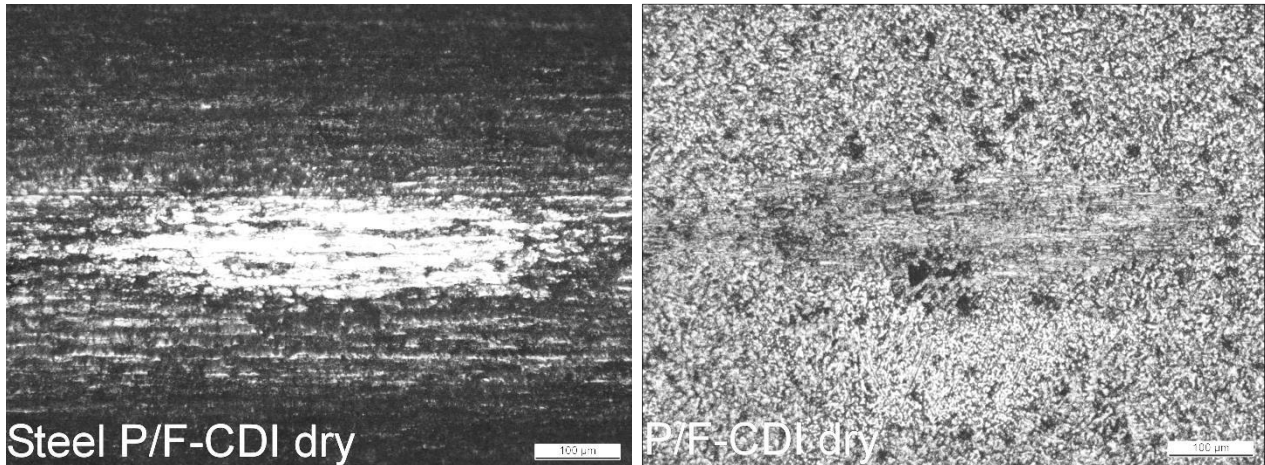
Fig. 25. Wear scar on the (left image) steel wire and the (right image) corresponding pearlitic-ferritic chill-cast SG iron disc sample after the test cycle without lubrication. The direction of motion of the steel wire sample was horizontal in the images.
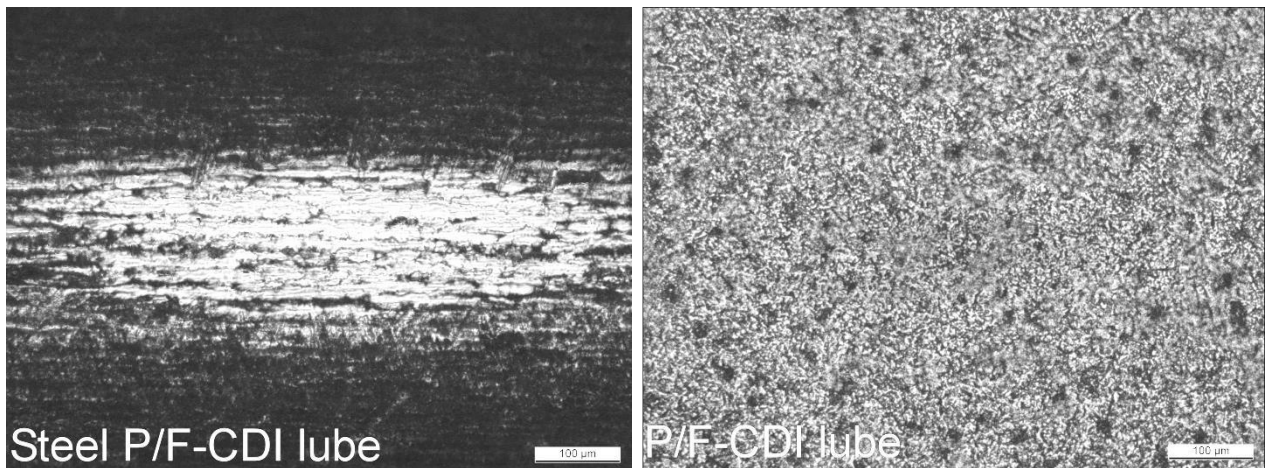
Fig. 26. Wear scar on the (left image) steel wire and the (right image) corresponding pearlitic-ferritic chill-cast SG iron disc sample after the test cycle with lubrication. The direction of motion of the steel wire sample was horizontal in the images.

Unlubricated contact of steel against pearlitic-ferritic chill-cast SG iron

The coefficient of static friction for steel against the pearlitic-ferritic CDI showed some scatter and a decreasing trend at higher loads. The average value for the coefficient of friction, $\mu=0.234$, was the highest among the combinations of materials and lubricating conditions studied in this work and close to that of the unhardened cast irons in unlubricated contact with steel wire. The wire and disc surfaces show traces of strong interaction, which is in agreement with the high level of the coefficient of friction. The surface of the pearlitic-ferritic CDI disc shows less clear graphite areas than what was seen on the SG irons, hence the availability of solid lubricant in the interface can be assumed as poor.

Lubricated contact of steel against pearlitic-ferritic chill-cast SG iron

The lubrication gave a strong reduction in the coefficient of static friction of the steel and P/F-CDI couple. On the cast iron disc, almost no wear marks were found. On the corresponding steel wire, a bright, polished area was found. The area of the wear surface on the steel wire slider from the lubricated test looks larger than that of the wire sample from the unlubricated test, while the latter had been subjected to more extensive mutations and appears to have been partially covered by a – possibly work hardened - transfer layer. In this test, the availability of graphite for the lubrication of the contact was as poor as under the unlubricated conditions, and therefore the reduction in the coefficient of static friction has to be addressed to the paraffinic vaseline.

Steel against P-CDI

Graphs showing the coefficients of static friction for steel wire against the pearlitic chill-cast SG iron at 9.6…96 N load, under unlubricated and petrolatum-lubricated conditions, respectively, are presented in the Figs. 27 and 28, and micrographs showing wear scars on the samples after the test cycles are presented in the Figs. 29 and 30.
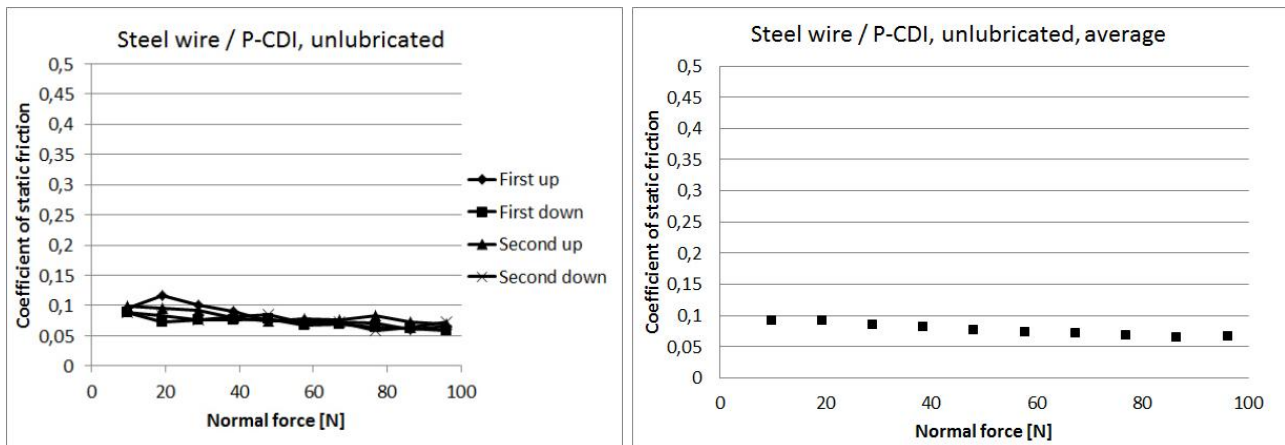
Fig. 27. Coefficients of static friction for unlubricated contact with steel wire against pearlitic chill-cast SG iron. The average value at 38.4...96 N load (26 measurement points) was μs=0.072±0.008.
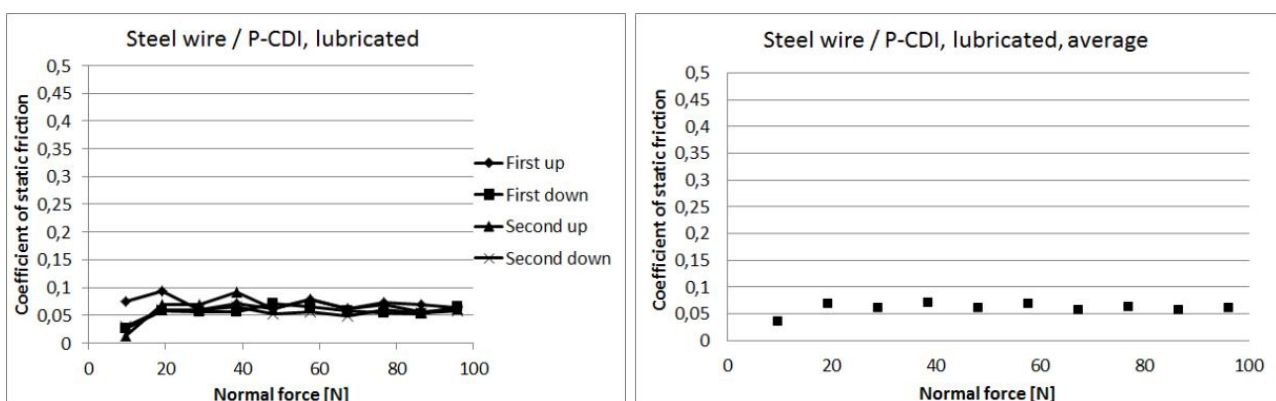
Fig. 28. Coefficients of static friction for a lubricated contact with steel wire against pearlitic chill-cast SG iron. The average value at 38.4...96 N load (26 measurement points) was μs=0.064±0.009.
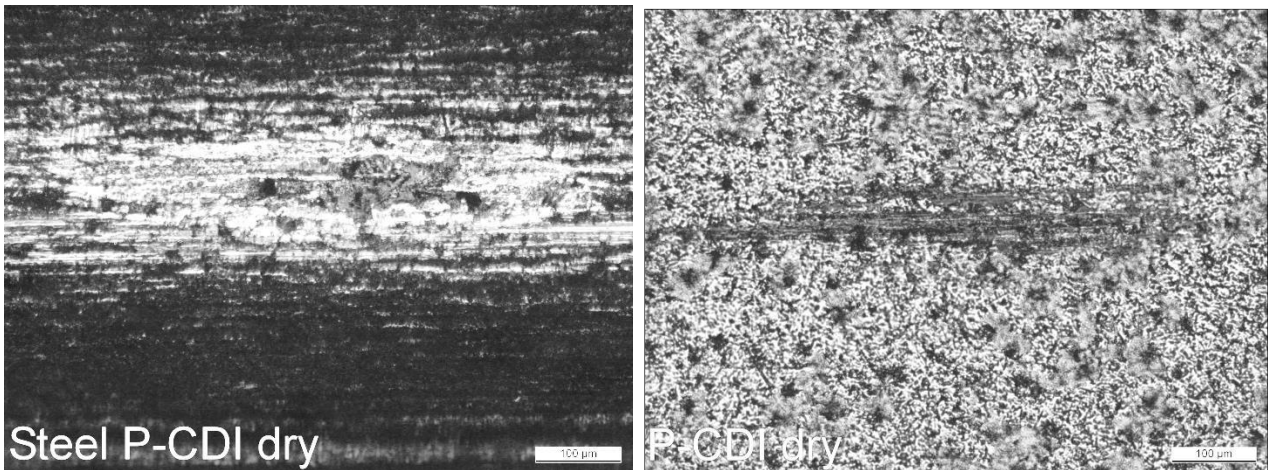
Fig. 29. Wear scar on the (left image) steel wire and the (right image) corresponding pearlitic chill-cast SG iron disc sample after the test cycle without lubrication. The direction of motion of the steel wire sample was horizontal in the images.
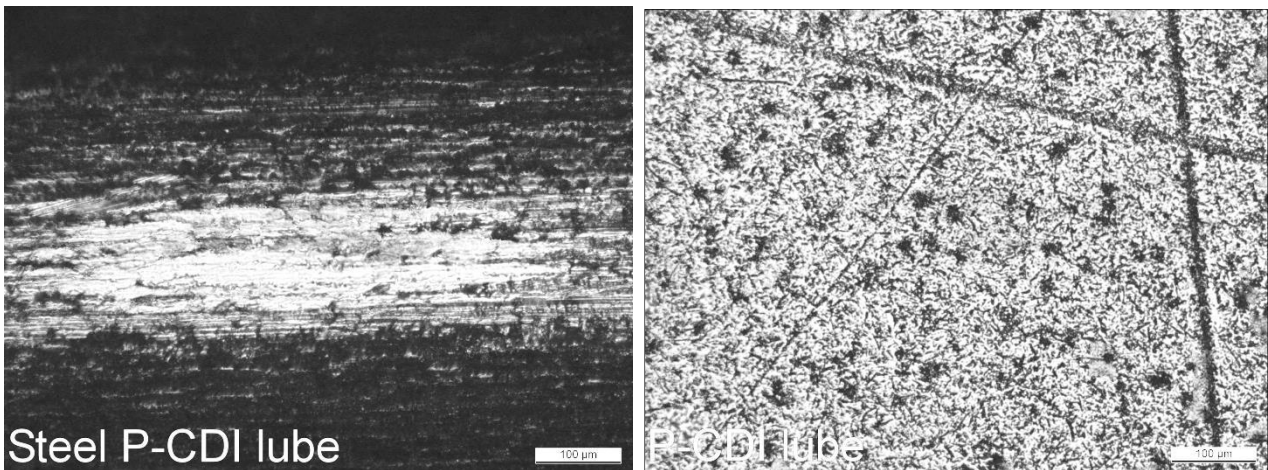
Fig. 30. Wear scar on the (left image) steel wire and the (right image) corresponding pearlitic chill-cast SG iron disc sample after the test cycle with lubrication. The direction of motion of the steel wire sample was horizontal in the images.

Unlubricated contact of steel against pearlitic chill-cast SG iron

Without lubrication, the pearlitic CDI showed a stable coefficient of friction of μ=0.072, which was the lowest value within the present group of unlubricated couples and similar to that obtained with the ADI and CrC materials without lubrication. Metal-to-metal interactions between the steel wire slider and the pearlitic CDI disc must, however, have occurred at some stage of the test cycle,

obvious from the surface images taken after the test. The transfer layer, which appears to have been formed on the steel slider, seems to have suppressed the wear of the steel surface, the area of which was not significantly larger than after the corresponding lubricated test.

Lubricated contact of steel against pearlitic chill-cast SG iron

The introduction of the chosen lubricant into the interface between the steel wire and P-

CDI disc surfaces furthermore lowered the coefficient of friction to the level μ=0.064, which was the lowest one in the present study. After the test cycle under the conditions of lubrication, no wear scars of significance were found on the P-CDI disc, while correspondingly the steel slider was mainly characterized by a shining contact surface. The coefficient of static friction for the steel and P-CDI combination was rather insensitive to the present two lubricating conditions.

Steel against thermal spray coated CrC-TS1

Graphs showing the coefficients of static friction for steel wire against the thermal spray coated CrC-TS1 at 9.6…96 N load, under unlubricated and petrolatum-lubricated conditions, respectively, are presented in the Figs. 31 and 32, and micrographs showing the wear scars on the samples after the tests are presented in the Figs. 33 and 34. On the thermal spray coated disc, no wear scar was found after the lubricated test sequence.
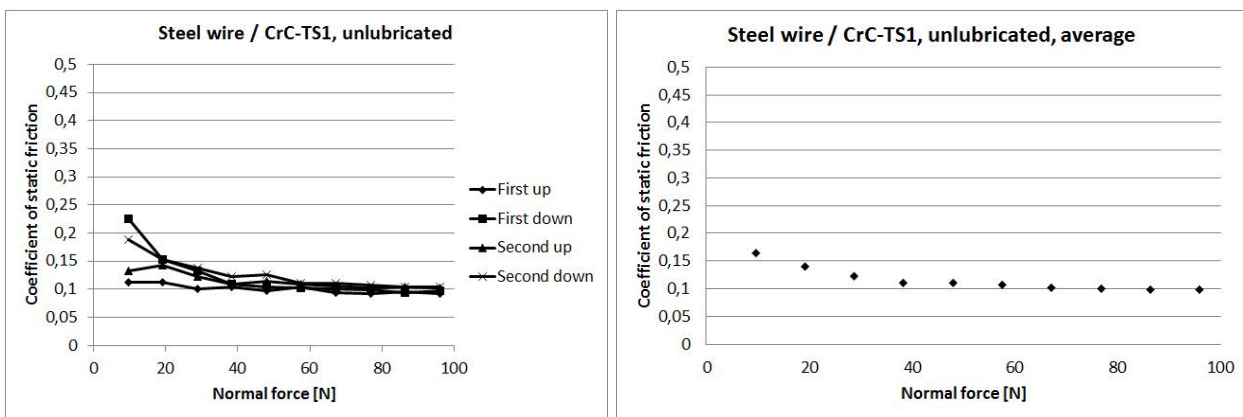
Fig. 31. Coefficients of static friction for unlubricated contact with steel wire against the thermal spray coated CrC-TS1 coating. The average value at 38.4...96 N load (26 measurement points) was μs=0.104±0.008.
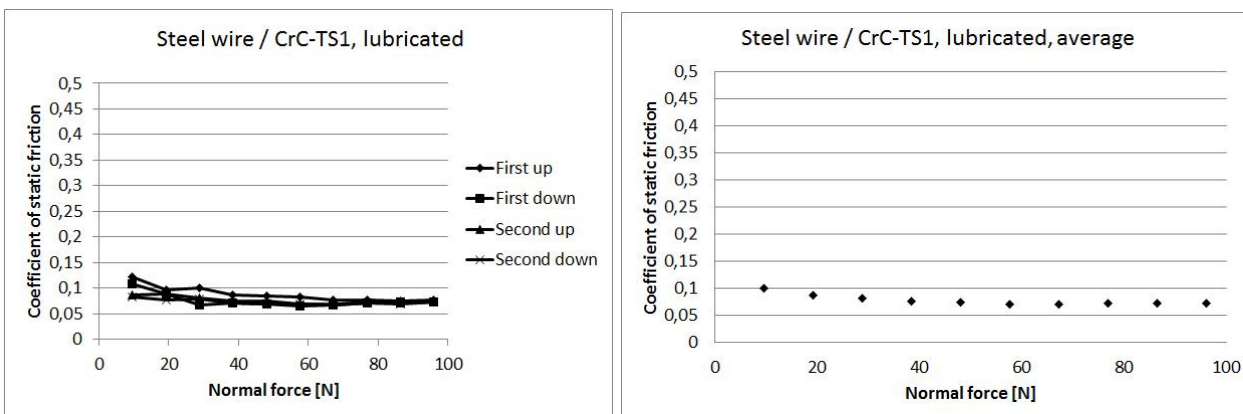
Fig. 32. Coefficients of static friction for a lubricated contact with steel wire against the thermal spray coated CrC-TS1 coating. The average value, valid for 38.4...96 N load (26 measurement points), was μs=0.073±0.005.
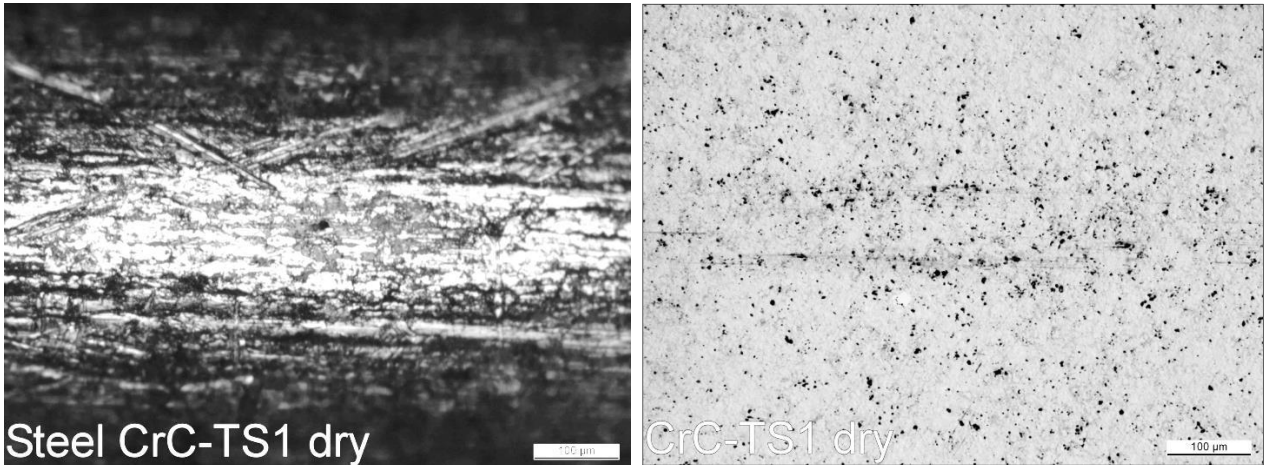
Fig. 33. Wear scar on the (left image) steel wire and the (right image) corresponding CrC-TS1 thermal spray coated sample after the test cycle without lubrication. The direction of motion of the steel wire sample was horizontal in the images.
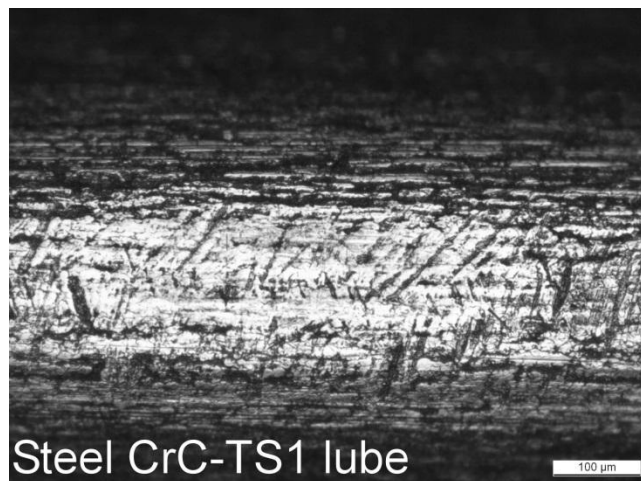
Fig. 34. Wear scar on the steel wire sample after the test cycle against the thermal spray coated CrC-TS1 coating with lubrication. On the disc surface, no marks from the measurements were visible. The direction of motion of the steel wire sample was horizontal in the image.

Unlubricated contact of steel against the commercial CrC-based thermal spray coating

For steel against the commercial CrC-TS1 coating without lubrication, the coefficient of static friction (μ=0.10) lied between the lowest and highest values for the unlubricated couples in this work, and was quite stable regardless of loads and number of sliding events. On the CrC coated disc, some ferrous deposits occurred after the test cycle, but no other surface alterations were observed on the disc. The wire surface alterations were mainly limited to polishing.

Lubricated contact of steel against the commercial CrC-based thermal spray coating

Lubrication decreased the level of the coefficient of static friction for steel on the

commercial CrC-TS1 coating to μ=0.073 and the level remained very stable during the test series. The steel wire surface became slightly polished by micro abrasion during the test cycle, but on the CrC coated disc the surface alterations had been so small that no wear scars could be detected under the light optical microscope.

Steel against thermal spray coated WC-TS2

Graphs showing the coefficients of static friction for steel wire against the thermal spray coated WC-TS2 at 9.6…96 N load, under unlubricated and petrolatum-lubricated conditions, respectively, are presented in the Figs. 35 and 36, and micrographs showing the wear scars on the test samples after the tests are presented in the Figs. 37 and 38. On the thermal spray coated disc, no wear scar was found after the lubricated test sequence.
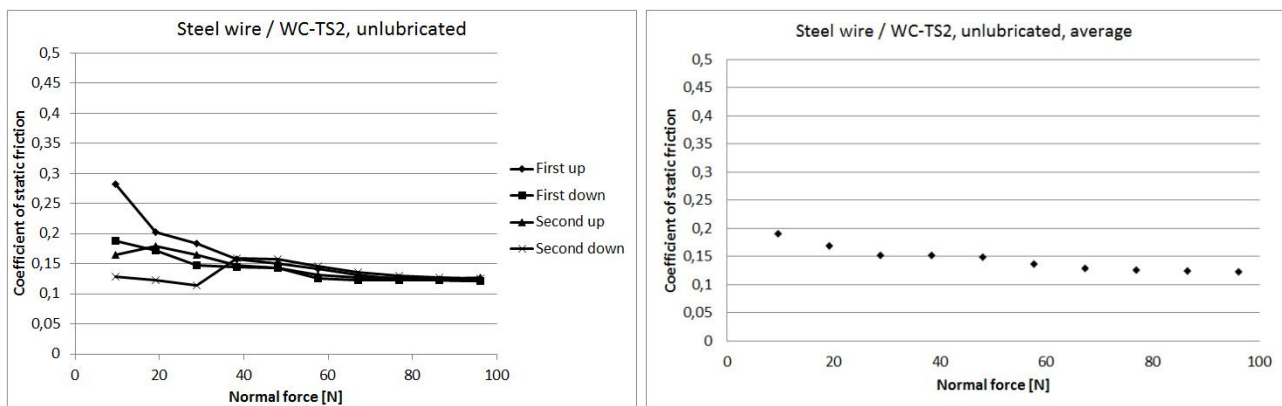
Fig. 35. Coefficients of static friction for unlubricated contact with steel wire against the thermal spray coated WC-TS2 coating. The average value at 38.4...96 N load (26 measurement points) was μs=0.134±0.012.
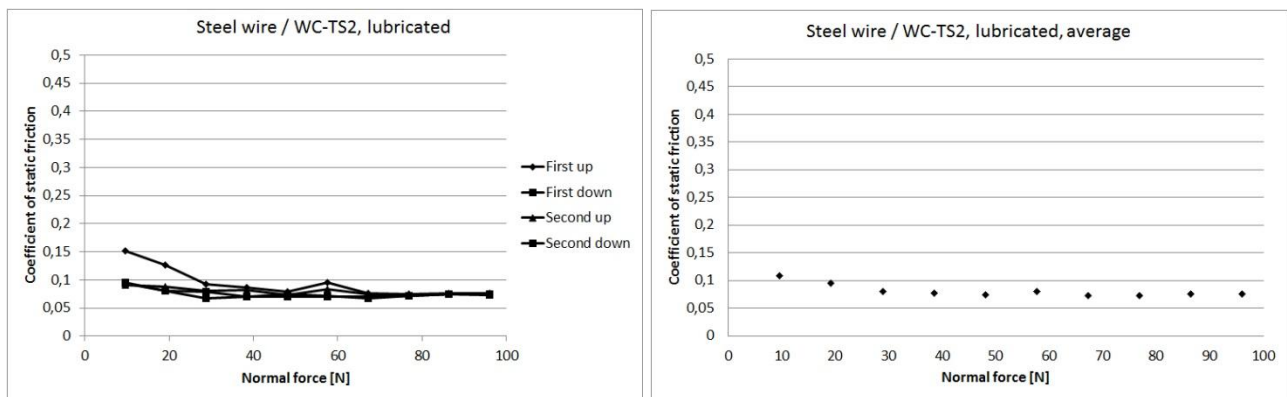
Fig. 36. Coefficients of static friction for a lubricated contact with steel wire against the thermal spray coated WC-TS2 coating. The average value at 38.4...96 N load (26 measurement points) was μs=0.075±0.006.
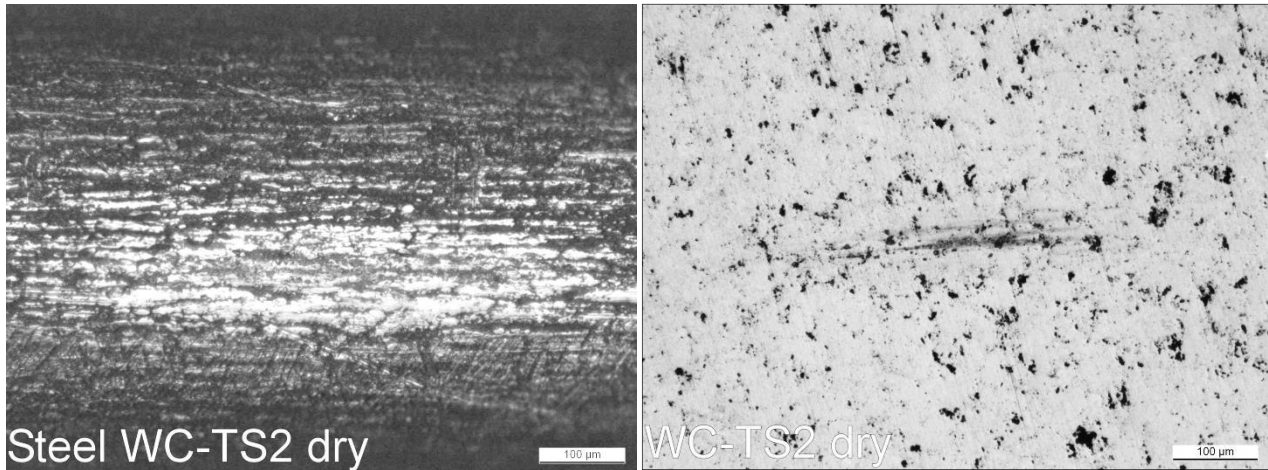
Fig. 37. Wear scar on the (left image) steel wire and the (right image) corresponding WC-TS2 thermal spray coated sample after the test cycle without lubrication. The direction of motion of the steel wire sample was horizontal in the images.
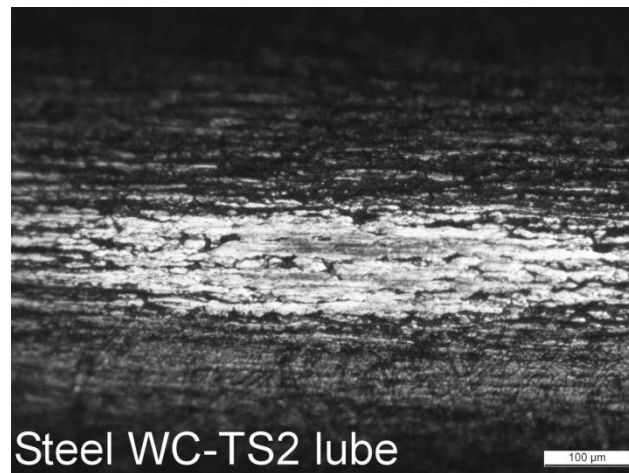
Fig. 38. Wear scar on the steel wire sample after the tests cycle against the thermal spray coated WC-TS2 coating with lubrication. On the disc surface, no traces from the measurements were visible. The direction of motion of the steel wire sample was horizontal in the image.

Unlubricated contact of steel against the WC-based thermal spray coating

When unlubricated, the tungsten carbide based cermet coating WC-TS2 gave a coefficient of static friction that was higher (μ=0.13) than that of the two CrC cermet coatings. The surface alterations on the steel wire slider and the WC coated disc strongly resembled those of the two unlubricated steel-CrC combinations, in particular in terms of the tiny scratches and the ferrous deposit spots on the disc.

Lubricated contact of steel against the WC-based thermal spray coating

With lubricant added, the coefficient of static friction for steel and WC fell to almost the same level (μ=0.075) as that of steel against the two CrC coatings when lubricated. On the WC disc, no wear marks were found by light

optical microscopy, and on the corresponding steel wire slider only a shining wear scar occurred.

Steel against thermal spray coated Mo-TS3

Graphs showing the coefficients of static friction for steel wire against the thermal spray coated Mo-TS3 coating at 9.6…96 N load, under unlubricated and petrolatum-lubricated conditions, respectively, are presented in the Figs. 39 and 40, and micrographs showing the wear scars on the test samples after the tests are presented in the Figs. 41 and 42. On the thermal spray coated disc, no wear scar was found after the lubricated test sequence.
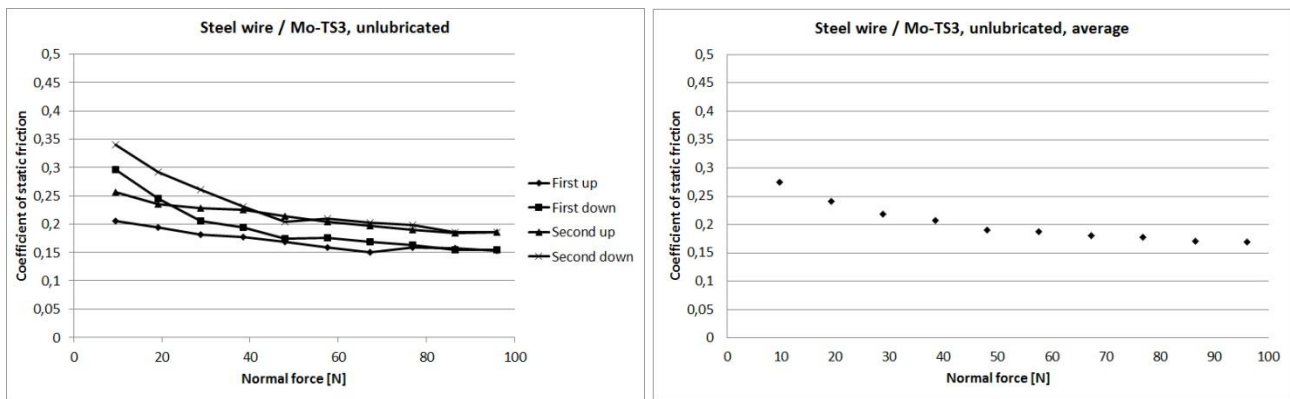
Fig. 39. Coefficients of static friction for unlubricated contact with steel wire against the thermal spray coated Mo-TS3 coating. The average value at 38.4...96 N load (26 measurement points) was µs=0.183±0.023.
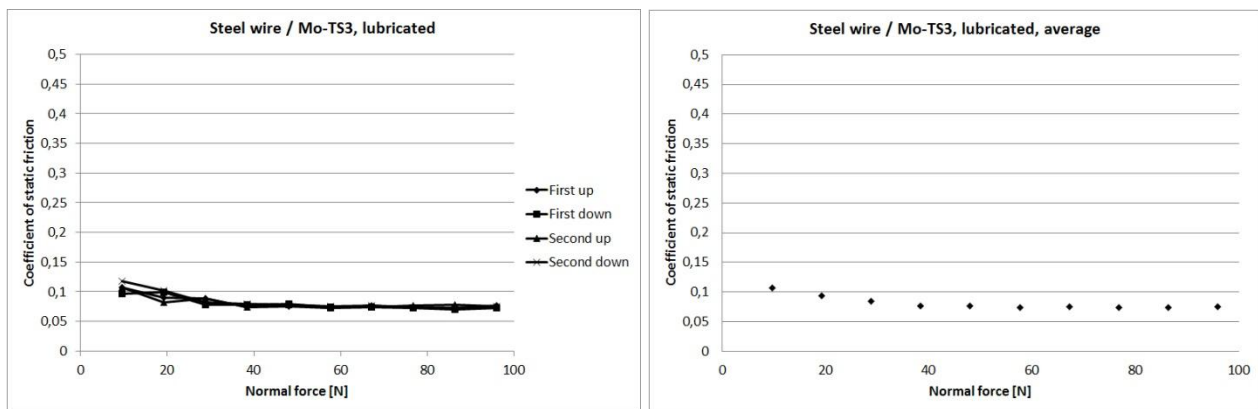
Fig. 40. Coefficients of static friction for a lubricated contact with steel wire against the thermal spray coated Mo-TS3 coating. The average value at 38.4...96 N load (26 measurement points) was µs=0.075±0.002.
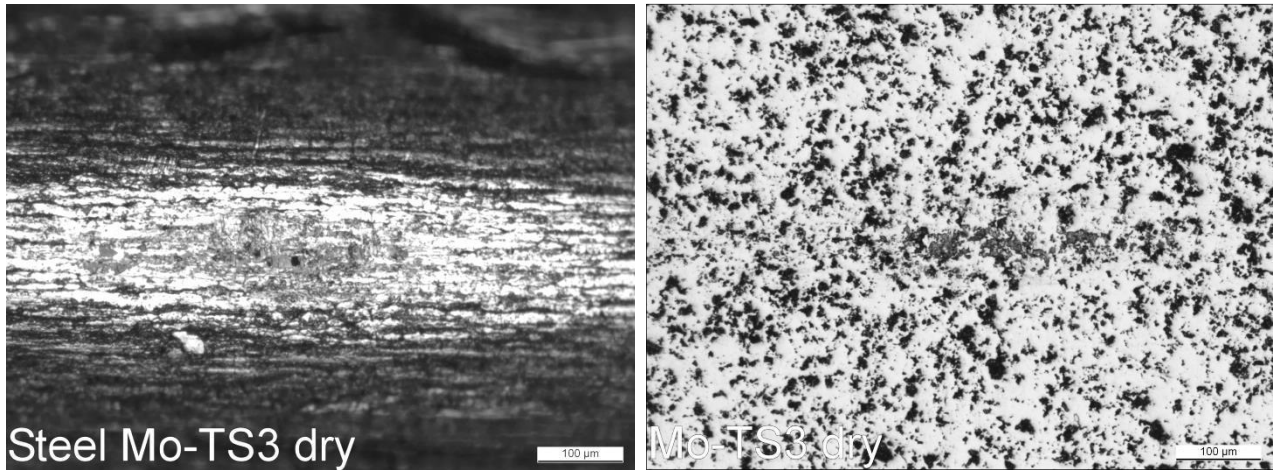
Fig. 41. Wear scar on the (left image) steel wire and the (right image) corresponding Mo-TS3 thermal spray coated sample after the test cycle without lubrication. The direction of motion of the steel wire sample was horizontal in the images.
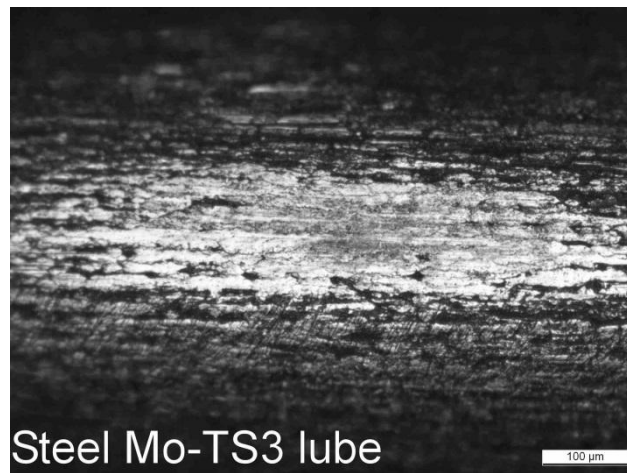
Fig. 42. Wear scar on the steel wire sample after the tests cycle against the thermal spray coated Mo-TS3 coating with lubrication. On the disc surface, no traces from the friction measurements were visible. The direction of motion of the steel wire sample was horizontal in the image.

Unlubricated contact of steel against the Mo-based thermal spray coating

Under dry conditions, the coefficient of static friction for the steel and Mo-TS3 couple was higher (μ=0.183) than for steel against the other four thermal spray coatings without lubrication. This could be explained by the surface roughness (Ra=0.18 µm) of the Mo coated disc, which was higher than that of the other four thermal spray coatings, but as will be seen below, the surface roughness as such

cannot be the sole reason for the high coefficient of static friction. As the result of the fairly strong tribological interactions, the contact surfaces of the steel wire slider and the Mo disc revealed tribolayers of adhesively attached material.

Lubricated contact of steel against the Mo-based thermal spray coating

The paraffinic vaseline reduced the coefficient of static friction for the steel and

Mo-TS3 couple (μ=0.075) to approximately the same level as that of the four other thermal spray coatings. The Mo coated disc did not reveal any marks from the sliding events. During the test cycle, the contact surface of the steel wire slider had been polished against the Mo coated disc surface.

Steel against thermal spray coated CrC-TS4

Graphs showing the coefficients of static friction for steel wire against the thermal spray coated CrC-TS4 at 9.6…96 N load, under unlubricated and petrolatum-lubricated conditions, respectively, are presented in the Figs. 43 and 44, and micrographs showing the wear scars on the test samples after the tests are presented in the Figs. 45 and 46. On the thermal spray coated disc, no wear scar was found after the lubricated test sequence.
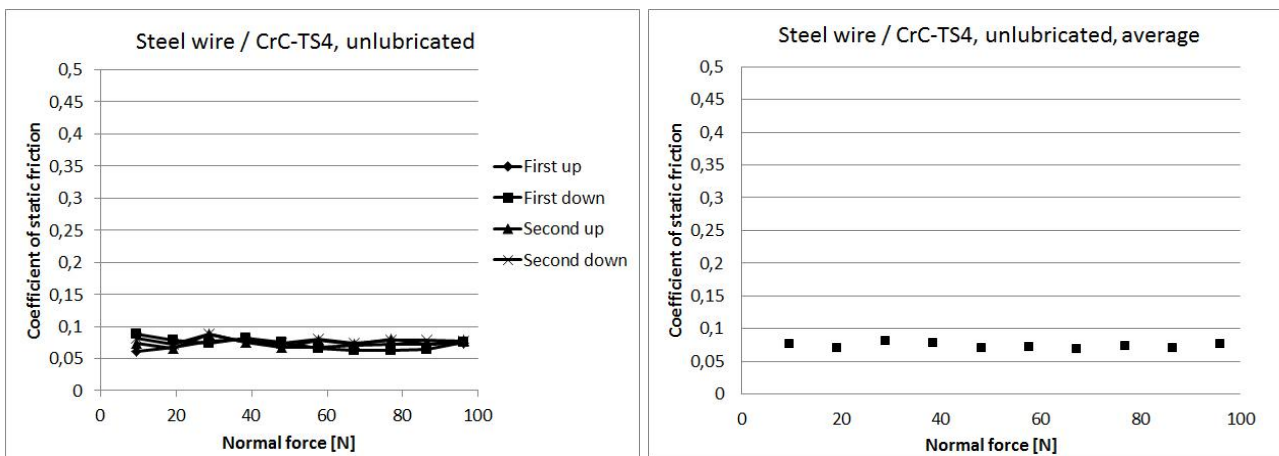
Fig. 43. Coefficients of static friction for unlubricated contact with steel wire against thermal spray coated CrC-TS4. The average value at 38.4...96 N load (26 measurement points) was μs=0.073±0.005.
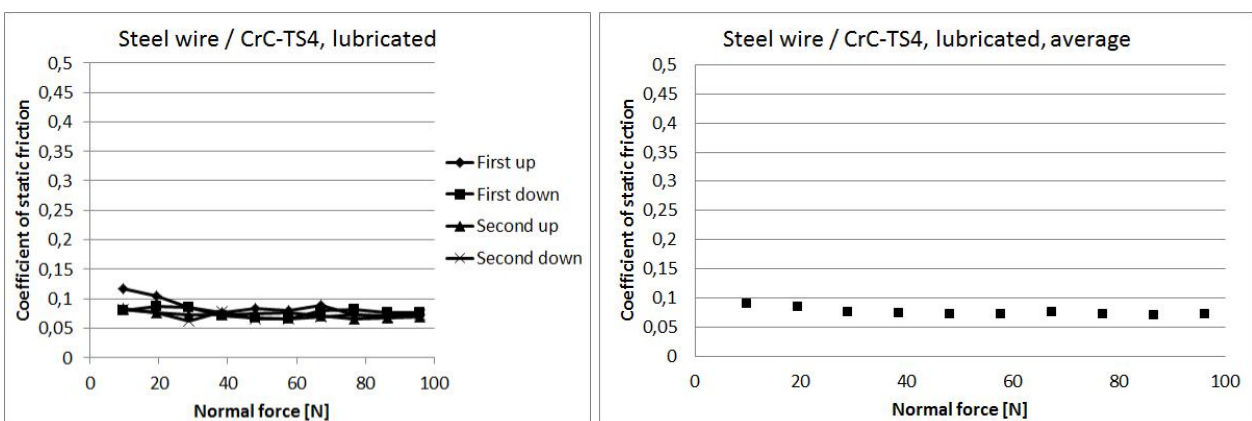
Fig. 44. Coefficients of static friction for a lubricated contact with steel wire against thermal spray coated CrC-TS4. The average value at 38.4...96 N load (26 measurement points) was μs=0.073±0.006.
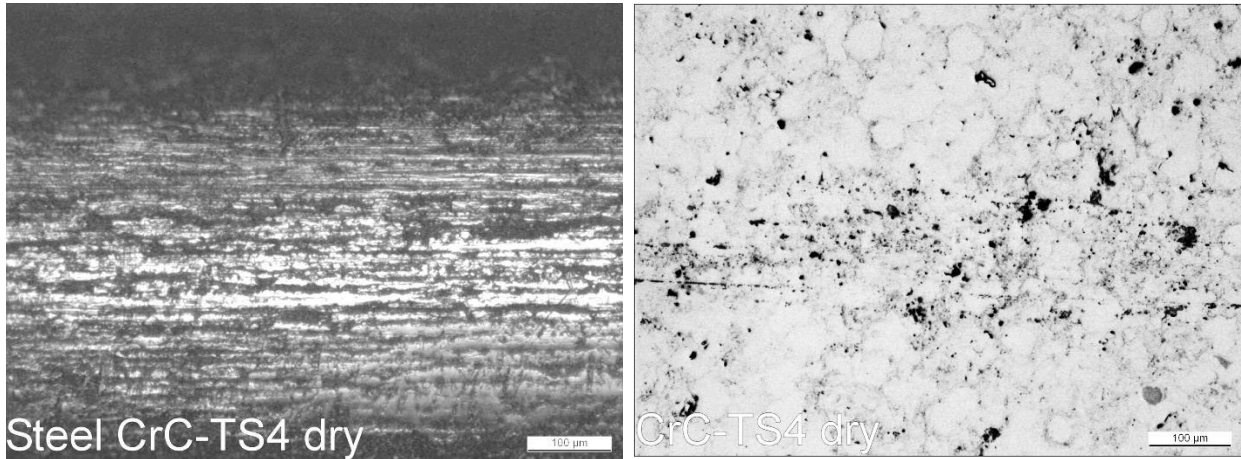
Fig. 45. Wear scar on the (left image) steel wire and the (right image) corresponding CrC-TS4 thermal spray coated sample after the test cycle without lubrication. The direction of motion of the steel wire sample was horizontal in the images.
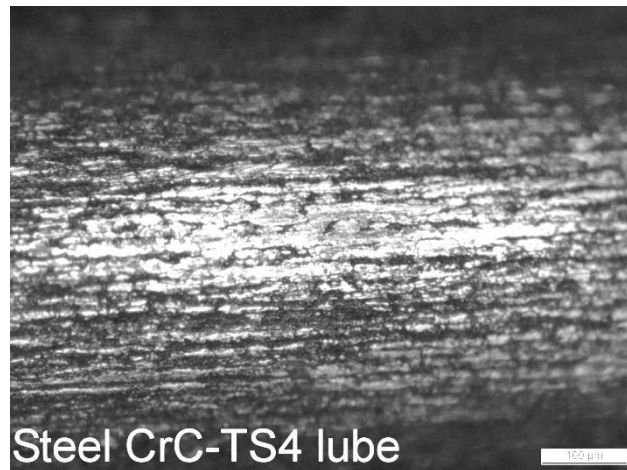
Fig. 46. Wear scar on the steel wire sample after the tests cycle against the thermal spray coated CrC-TS4 coating with lubrication. On the disc surface, no marks from the measurements were visible. The direction of motion of the steel wire sample was horizontal in the image.

Unlubricated contact of steel against the experimental CrC-based thermal spray coating

The coefficient of static friction for steel wire against the experimental CrC-TS4 coating with no lubricant applied was as low as μ=0.073, and the value remained almost the same during the entire test cycle. Tiny scratches and some ferrous deposits characterized the sliding track on the CrC disc surface, while the steel wire revealed a shining contact surface.

Lubricated contact of steel against the experimental CrC-based thermal spray coating

The introduction of the lubricant into the steel and CrC-TS4 interface did practically not affect the coefficient of static friction, which also in this case was μ=0.073. The wear was, however, reduced by the lubricant, as on the

CrC disc surface no wear track was visible under the light optical microscope.

Steel against thermal spray coated VC-TS5

Graphs showing the coefficients of static friction for steel wire against the thermal spray coated VC at 9.6…96 N load, under unlubricated and petrolatum-lubricated conditions, respectively, are presented in the Figs. 47 and 48, and micrographs showing the wear scars on the samples after the test cycle are presented in the Figs. 49 and 50. On the thermal spray coated disc, no wear scar was found after the lubricated test sequence
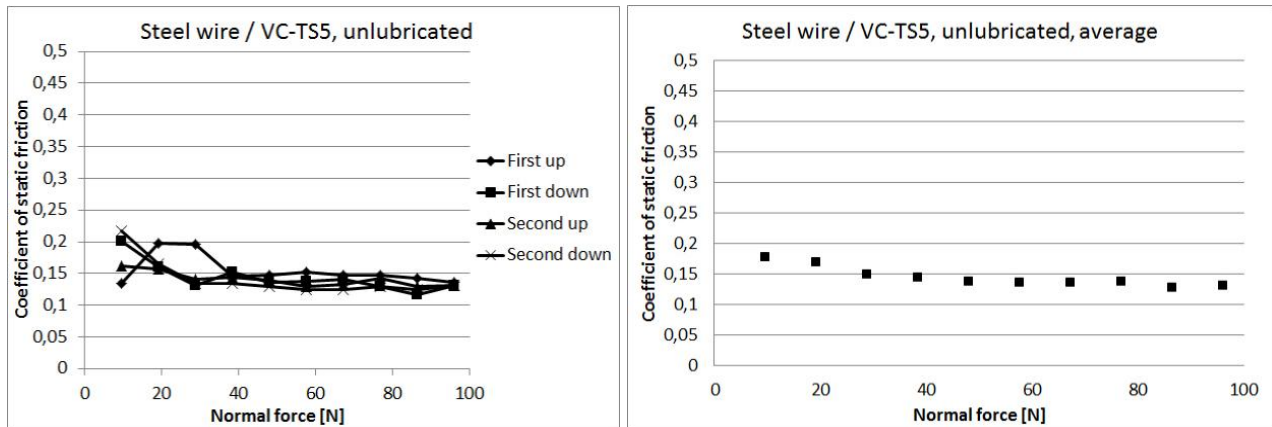
Fig. 47. Coefficients of static friction for unlubricated contact with steel wire against thermal spray coated VC. The average value at 38.4...96 N load (26 measurement points) was $\mu s=0.136\pm0.009$.
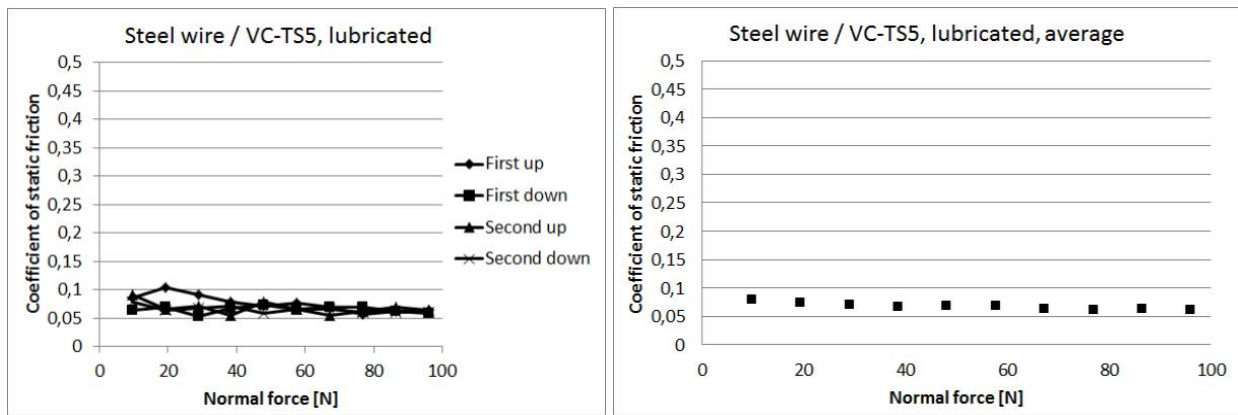
Fig. 48. Coefficients of static friction for a lubricated contact with steel wire against thermal spray coated VC. The average value at 38.4...96 N load (26 measurement points) was $\mu s=0.066\pm0.006$.
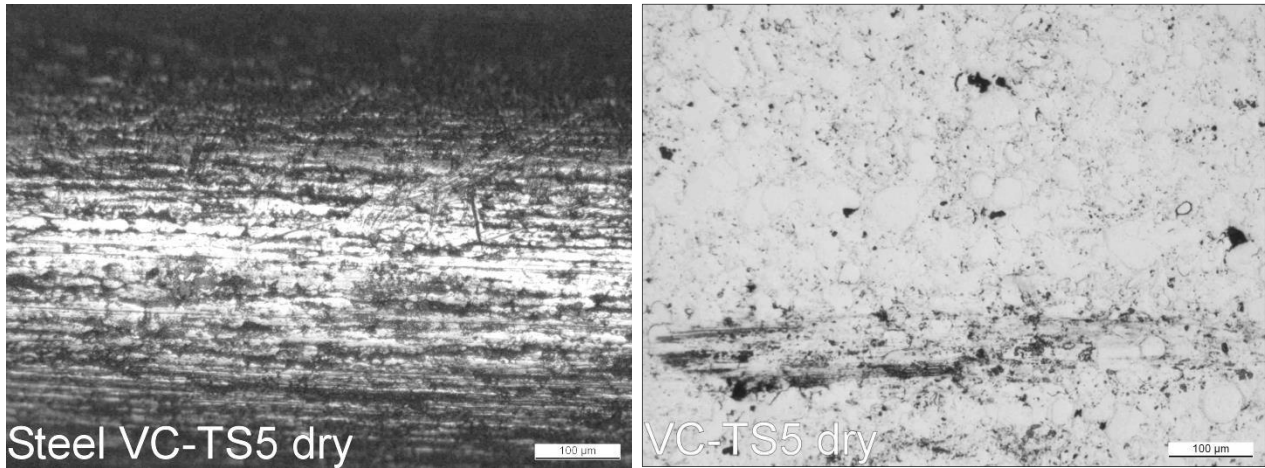
Fig. 49. Wear scar on the (left image) steel wire and the (right image) corresponding VC-TS5 thermal spray coated sample after the test cycle without lubrication The direction of motion of the steel wire sample was horizontal in the images.
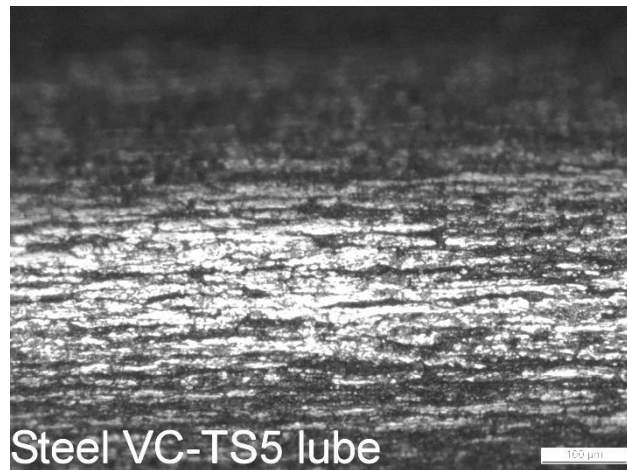
Fig. 50. Wear scar on the steel wire sample after the tests against the thermal spray coated VC-TS5 coating with lubrication. On the disc surface, no marks from the measurements were visible. The direction of motion of the steel wire sample was horizontal in the image.

Unlubricated contact of steel against the VC-based thermal spray coating

Under unlubricated sliding conditions, the coefficient of static friction for steel against the VC coating stayed on a fairly stable level of µ=0.14 during the test cycle. The relatively high coefficient of friction correlates with the tiny scratches and the patches of a thin, ferrous transfer layer that characterized the sliding surface on the VC-coated disc after the test cycle.

Lubricated contact of steel against the VC-based thermal spray coating

The application of the lubricant into the sliding interface reduced the coefficient of static friction for steel wire and the VC coating to µ=0.066, which is among the lowest values within the present experimental investigation. Under lubrication, no visible patches of a transfer layer were formed on the sliding track of the VC coated disc.

Figure 51 summarizes the average values of the present, measured coefficients of static friction within the normal force interval 35-100 N. In the Figures 52 and 53, the development in the average value for the coefficient of friction within the normal force interval 35-100 N is shown for the unlubricated and lubricated sliding conditions, respectively.
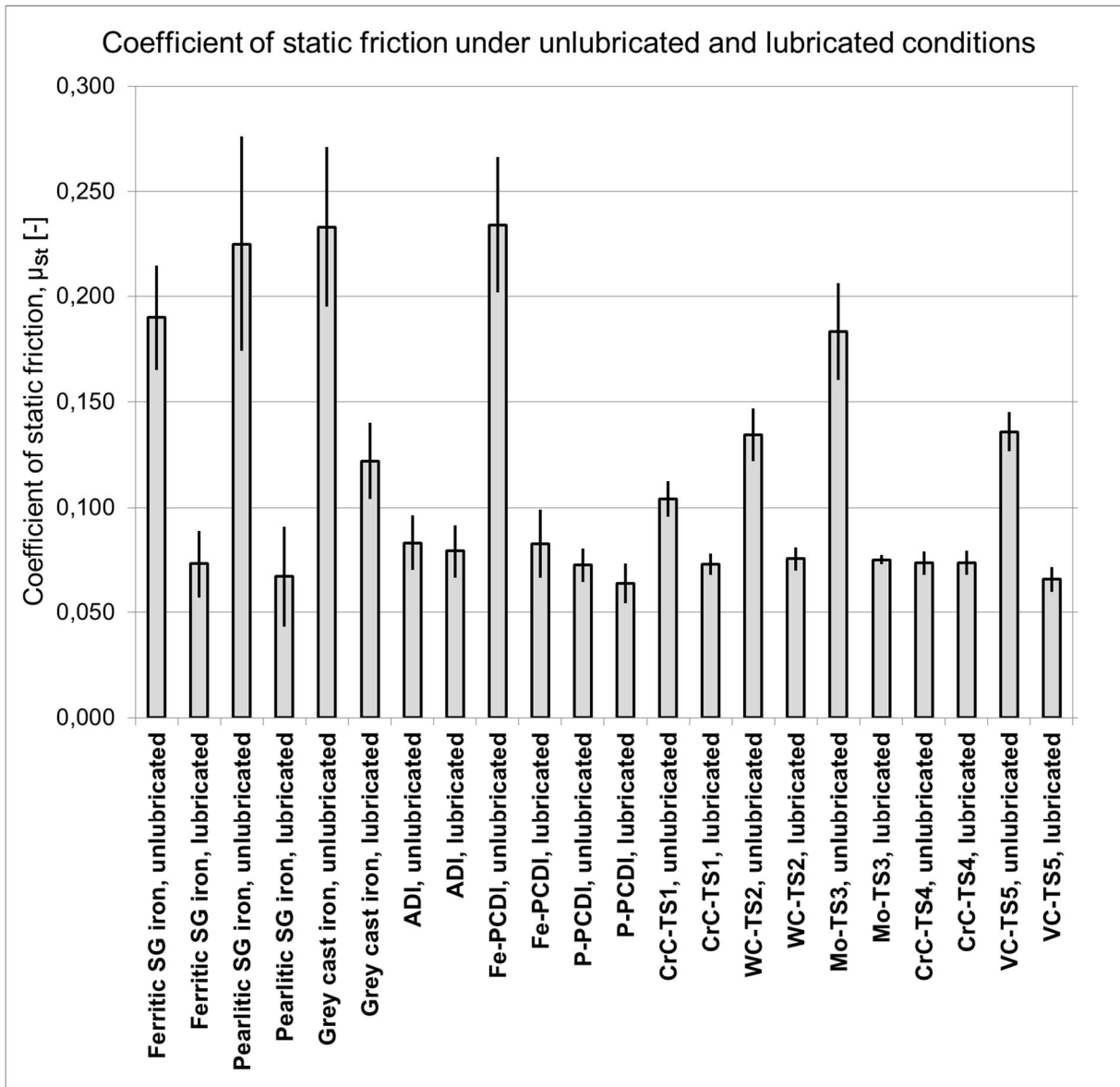
Fig. 51. Graphical summary of the average values for the coefficients of static friction measured under 35-100 N normal force in the present work. The vertical bar at the upper end of each column indicates the standard deviation of the average value.
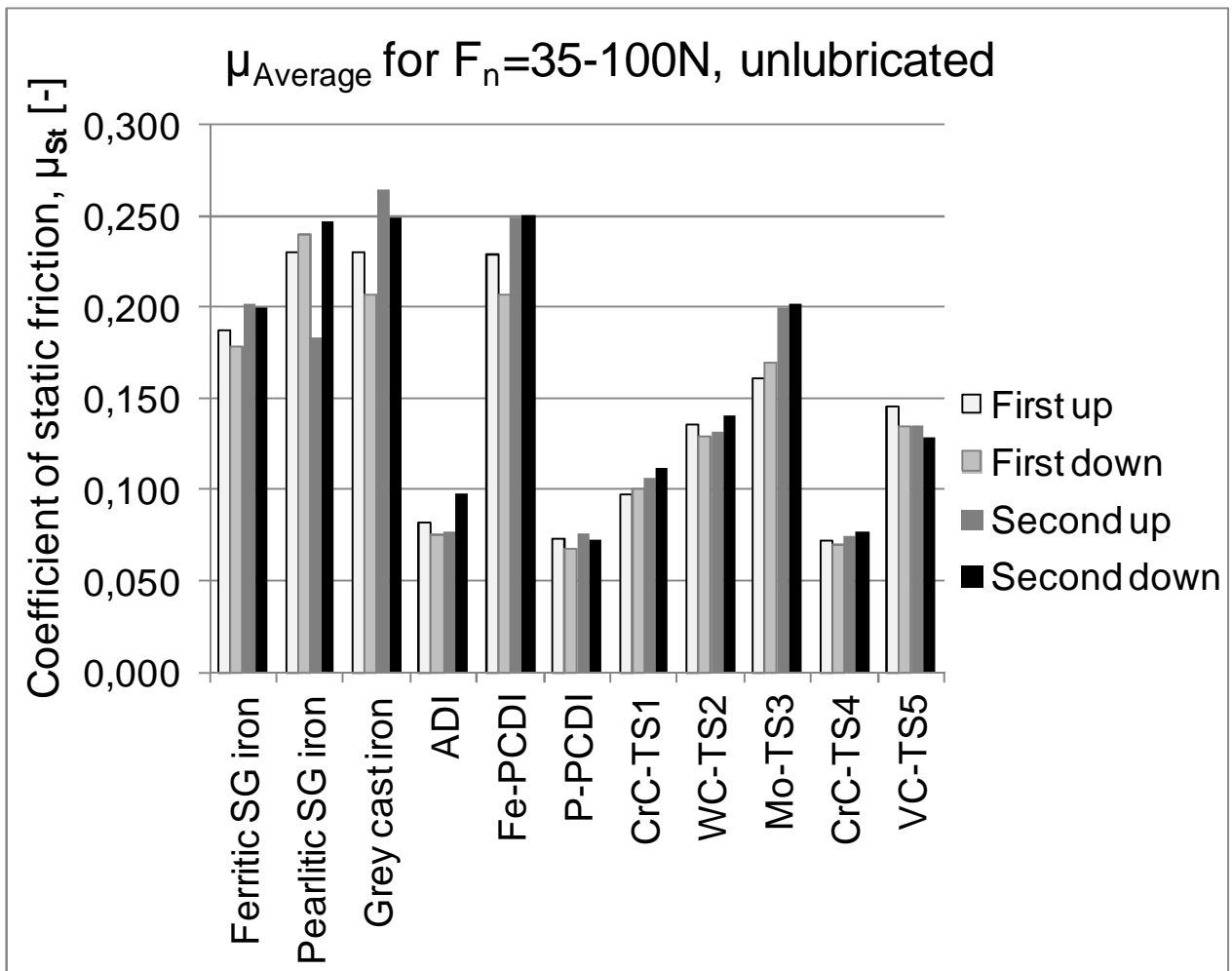
Fig. 52. The development in the average value for the coefficient of friction within the normal force interval 35-100 N under unlubricated sliding conditions.
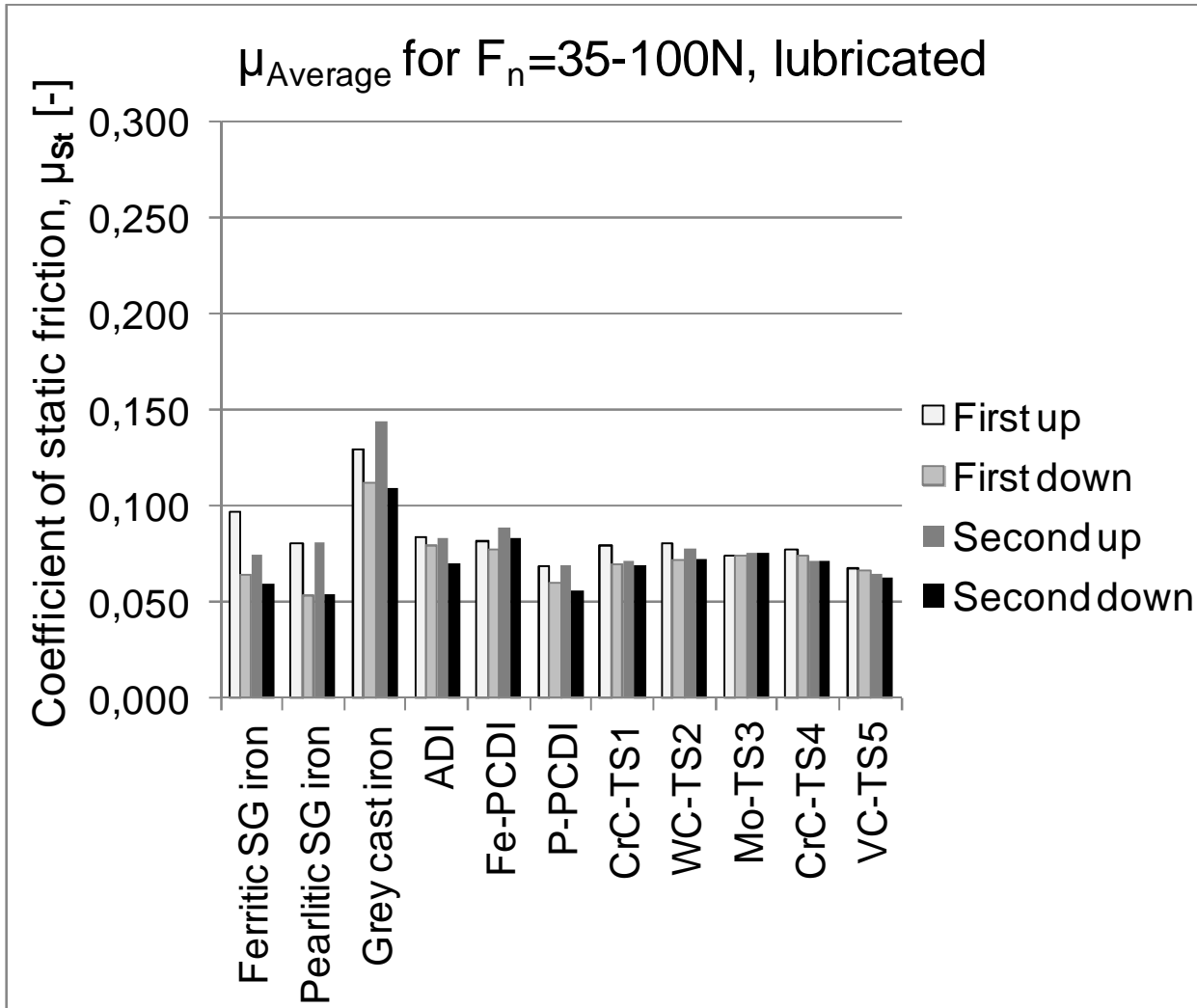
Fig. 53. The development in the average value for the coefficient of friction within the normal force interval 35-100 N under lubricated sliding conditions.

DISCUSSION

High-friction and low-friction material pairs

A feature in common of all the tests with steel wire against cast iron was that the coefficient of static friction was higher at low loads than at higher loads. The reason for the decrease in the coefficient of static friction with load would require further studies. One possible explanation is that the surface roughness, abrasion and a tendency for plowing friction plays a relatively greater role as long as the normal force is low. Furthermore, at higher contact pressure and increasing elastic-plastic deformation of the iron matrix that surrounds the graphite spheres or lamellae, the squeezing-out of near-surface graphite from the iron matrix and the formation of distributed graphite film patches can be assumed to offer friction reduction [5, 6].

The overviews of the static coefficients of friction for the present material pairs and lubrication conditions show a large variation, with average values ranging from $\mu=0.07$ to $\mu=0.23$. The lowest average static coefficients of friction were obtained for steel wire in

contact with the ADI, the PCDI and the CrC-coated plate materials, both lubricated and unlubricated. The highest average static coefficients of friction were obtained in the unlubricated tests with grey cast iron, Fe-PCDI and SG iron plates, in the unlubricated tests with the Mo, VC and WC coated plates and in the lubricated tests with grey cast iron plates.

The reason for the large differences in the static coefficients of friction is a complex combination of chemical and physical factors. Among these, the chemical affinity, or the lack of it, between the steel wire and the respective plate materials is a dominating effect, often referred to as the adhesion between materials. According to early work by Bowen and Tabor [7], and by Rabinowicz [8], the tendency of the mating surfaces to form chemical joints largely determines the coefficient of friction. In the case of the ferrous metal plates and the metal-coated plates, with the exception of the ADI and PCDI plates, iron-to-iron joints can be assumed as at least partly responsible for the high static coefficients of friction in the unlubricated and even in the lubricated contacts.

The dominating physical effect that affects the static coefficient of friction is the resistance against plowing (or the onset of plowing, as the present work is dealing with static friction). Softer materials, like the present grey and SG irons, show a tendency to higher friction forces due to plowing, while the hardest materials, like the present CrC-coatings, lead to lower plowing forces. Recent static friction tests by Dunn and co-workers, with steel against steel prepared for different surface roughness have shown that rougher surfaces lead to higher static coefficients of friction than do smoother surfaces, due to interlocking of topographical features in the rougher surfaces and the additional forces needed to shear the joints and to cause scratches [9].

The standard deviation values of the average static coefficients of friction seem to have a tendency to increase with the level of the coefficient of friction, most likely because the high average values are formed from both high and low values, while the low average values are mainly formed from low values only. This may reflect the fact that a high coefficient of friction causes more severe changes to the contact surface than does a low coefficient of friction in a similar situation.

When comparing the tribological behavior of the two present combinations of steel wire and CrC coated discs, with each other and with the other present material combinations, it becomes obvious that this type of coating can offer a low coefficient of static friction and contact surfaces that are not largely affected by the contacting events within the load and contact pressure levels studied.

Benefit from lubrication by paraffinic petrolatum

For all the material pairs of the present study, except for that comprising the CRC-TS4 coating, the static coefficient of friction was lower in the lubricated tests than in the unlubricated ones. As shown in the overviews of the Figures 51-53, the lubricant not only reduced the average static coefficient of friction, but also reduced the differences between the material combinations. The reducing and equalizing effect most likely comes from a reduction in the adhesion, due to the interlayer that was physically introduced between the steel wire and the plate sample surfaces. Due to the lack of additives in the petrolatum lubricant, and due to the low sliding velocity in the sliding contacts, chemical interactions between the lubricant or its constituents and the sliding surfaces are less pronounced.

While a minute amount of the present, additive-free paraffinic lubricant was sufficient to prevent adhesive wear and tribolayer formation on all of the tribological contact surfaces studied, the tests without lubrication caused the formation of tribolayers on the contact surfaces even at the present low sliding velocities and short sliding distances.

The ability of the lubricant to suppress the alterations in the tribological contact surfaces during the tests is reflected by the magnitude of the standard deviation bars in the bargraph (Figure 51) for the average static coefficients of friction, or the scatter in the measurements, which in general was lower in the lubricated tests. The lowest standard deviation levels occurred with the wire/coating combinations when lubricated, probably because the wear and the surface roughness alterations in these cases remained minute.

In the present petrolatum-lubricated tests, the recorded coefficients of static friction for steel against the three cast iron grades were partially higher than the results presented by Hwang and Zum Gahr for a hardened, polished steel ball in contact with a hardened, ground steel plate under lubrication by a mineral oil [10]. However, the present initial value (μs=0.15) for the coefficient of static friction at lubricated conditions is close to that presented by Bowden and Tabor in the Appendix of Ref. [7], which states μs=0.21 for a steel against a cast iron under lubrication with mineral oil.

The benefit of the lubrication can be seen in the influence of the subsequent loading cycles on the average value for the static coefficient of friction. For most of the unlubricated sliding couples, the average value for the static coefficient of friction increased with the number of sliding cycles, as shown in Figure 52. In the lubricated tests, however, the average value for the static coefficient of friction of most of the sliding couples was

decreased, see Figure 53, most likely owing to a beneficial running-in effect in the presence of the lubricant.

Possibly because of the relatively high surface roughness of the grey cast iron disc, wear marks of significant size were formed on the steel wire and cast iron disc samples during the petrolatum lubricated measurements. On the steel wire surface, a shining flat with numerous tiny scratches had been formed, probably due to an abrasive action by the roughness of the cast iron surface through the thin lubricant film. As a consequence of the interaction, the peaks of the disc surface roughness seem to have been abraded by the steel wire, in addition the formation of scratches in the direction of the measurements.

CONCLUSIONS

- For drawn, high-strength steel wire against the present counter materials, the coefficient of static friction without lubrication ranged from μ=0.07 to μ=0.23, and under petrolatum-lubricated conditions, the corresponding values were about μ=0.06 to μ=0.12. A minor effect of the surface roughness on the coefficient of friction was identified.
- Among the material combinations studied, the highest values for the coefficient of static friction were obtained with the two nodular cast iron grades, the grey cast iron and the pearlitic-ferritic chill-cast SG iron in unlubricated contact with the steel wire.
- Low values for the coefficient of static friction against steel wire were obtained under lubricated conditions with all the disc materials except the grey cast iron. Consequently, the highest values for the coefficient of static friction, both lubricated and unlubricated, were obtained when the steel wire was in contact with grey cast iron.

- Low and stable coefficients of static friction against steel wire, both lubricated and unlubricated, were obtained with ADI, pearlitic chill-cast SG iron and CrC as counter material. The latter indicates the benefit of using this type of coating as a surface engineering method for cast iron.

- In the unlubricated tests, transfer of material from one counter-surface to another occurred even at the present low velocities and short sliding distances. The performance of the additive-free, paraffinic lubricant was sufficient for preventing adhesive wear and materials transfer in this study.

ACKNOWLEDGEMENTS

REFERENCES

1. Jost, H. P. (Ed.). Lubrication (Tribology), Education and research, A report on the present position and indystry's needs. London, UK, 1966, Her Majesty's Stationary Office, 80 p.
2. Bhusan, B. (ed.). Modern tribology handbook, volume one, principles of tribology. Boca Raton, FL, USA, 2001, CRC Press LLC, 765 p.
3. Rabinowicz, E. Friction coefficient of noble metals over a range of loads. Wear, 1992, 159, 89-94.
4. Dunkin J.E. and Kim D.E. Measurement of static friction coefficient between flat surfaces. Wear, 1996, 193, 186-192.
5. Quanshun Luo, Jingpei Xie and Yanpei Song, Effects of microstructures on the abrasive wear behaviour of spheroidal cast iron. Wear, 1995, 184 (1), 1-10.
6. Ben Tkaya, M., Mezlini, S., El Mansori, M. and Zahouani, H. On some tribological effects of graphite nodules in wear mechanism of SG cast iron: Finite element and experimental analysis. Wear, 2009, 267 (1-4), 535-539.
7. Bowden, F. P. and Tabor, D. The friction and lubrication of solids, Part I. Oxford, UK, 1971, at the Clarendon Press, 374 p.
8. Rabinowicz, E. Determination of the compatibility of metals through static friction tests. ASLE Trans., 1971, 14 (3), 198-205.
9. Dunn, A., Wlodarczyk, K.L., Carstensen, J.V., Hansen, E.B., Gabzdyl, J., et al. Laser surface texturing for high friction contacts. Appl. Surf. Sci, 2015, in press.
10. Hwang, D.-H. and Zum Gahr, K.-H., Transition from static to kinetic friction of unlubricated or oil lubricated steel/steel, steel/ceramic and ceramic/ceramic pairs. Wear, 2003, 255, 365–375.